universität wien

MASTERARBEIT

Titel der Masterarbeit

„Characterization of Nrl1 protein in *Schizosaccharomyces pombe*“

verfasst von

David Fima Ruchman.

angestrebter akademischer Grad

Master of Science (MSc)

Wien, 2016

Studienkennzahl lt. Studienblatt	A 066 087
Studienrichtung lt. Studienblatt	Masterstudium Genetik und Entwicklungsbiologie
Betreut von / Supervisor:	Dr. Renee Schroeder
Mitbetreut von / Co-Supervisor:	Dr. Lucia Aronica

FUNDING

This work was supported by the Austrian Science Fund (FWF) [T527-B11 to LA; F43-08 to RS, F43-P10 to AB]; by the Medical Research Council [MC_PC_12003 to TK and TH]; by the Slovak
Research and Development Agency and Scientific Grant Agency [APVV-0111-12, 2/0014/14 to LC]; by the National Institute of Health [R01-GM059321 to SLF]. The data deposition to the Proteome Xchange Consortium was supported by PRIDE Team, EBI.

ABSTRACT

The fission yeast *Schizosaccharomyces pombe*, is an ideal model organism to study eukaryotic cell biology as it is easy to manipulate while sharing many features in common with higher organisms like centromeres with repetitive sequences, large replication origins, conserved telomere proteins, conserved heterochromatin proteins and epigenetic silencing mechanisms.

In this study the evolutionarily conserved Nrl1 protein in *S. pombe* has been characterized, and its role in pre-mRNA splicing and genome stability was identified. It is shown that, unlike its orthologue NRDE-2 in *C. elegans*, Nrl1 is not required for RNAi silencing and regulation of PolII elongation. Instead, Nrl1 forms a complex with splicing and mRNA processing factors and its deletion leads to significant changes in splicing patterns at several genomic loci. Furthermore, it is shown that nrl1Δ mutants exhibit features of endogenous DNA damage, such as elongated cell morphology and chromatin hypercondensation, along with defects in chromosome segregation during meiosis. Since Nrl1 does not physically associate with any protein involved in chromosome segregation and meiosis, the latter phenotype is likely the consequence of indirect effects of Nrl1 on gene expression and or splicing. In line with this hypothesis it has been found that Nrl1 deletion results in deregulation of key meiotic genes like the meiotic master regulator Mei2 and the meiosis-specific kinetochore factor Moa1, among others.

Altogether, these findings provide new functional insight into the role of the protein Nrl1 in pre-mRNA splicing and genome stability. Since Nrl1 is conserved in higher eukaryotes including humans, the significance of this study reaches beyond the yeast system. As a matter of fact, the human orthologue of Nrl1, hNRDE-2, is downregulated and associated with Copy Number Aberrations in tumor cells suggesting that it may act as a tumor suppressor. Our findings provide therefore the groundwork for future investigations on a possible role of hNRDE in cancer.

ZUSAMENFASSUNG

Die Spalthefe *Schizosaccharomyces pombe*, ist ein idealer Modellorganismus um eukaryotischen Zelle Biologie zu studieren, da es leicht zu manipulieren, während viele Gemeinsamkeiten mit höheren Organismen wie Zentromeren mit repetitiven Sequenzen, große Replikationsursprünge, konserviert Telomerproteine, konserviert Heterochromatin Proteine und epigenetische Silencing-Mechanismen.

In dieser Studie die evolutionär konserviert Nrl1 Protein in *S. pombe* charakterisiert würde und seine Rolle in pre-mRNA-Splicing und Genomstabilität identifiziert war. Es ist gezeigt, dass, im Gegensatz zu seinen Ortholog NRDE-2 in *C. elegans*, Nrl1 nicht für RNAi-Silencing und Regulierung der PolII Dehnung erforderlich ist. Stattdessen bildet Nrl1 einen Komplex mit Splice- und mRNA Verarbeitungsfaktoren und deren Löschung führt zu erheblichen Veränderungen in der Splicing-Muster an mehreren genomischen Loci. Darüber hinaus es ist gezeigt, dass nrl1Δ Mutanten zeigen Merkmale von endogenen DNA-Schäden, wie längliche Zellmorphologie und Chromatin Schwitz-, zusammen mit Defekten in der Chromosomensegregation während der Meiose. Da Nrl1 physisch nicht mit jedem Protein in der Chromosomensegregation und Meiose beteiligt assoziieren, ist dieser Phänotyp wahrscheinlich die Folge der indirekten Auswirkungen der Nrl1 auf die Genexpression und oder Splicing. Im Einklang mit dieser Hypothese es war gefunden, dass Nrl1 Löschung führt zu Deregulierung der Schlüssel Meiose Gene wie der Meiose Master-Regulator Mei2 und der Meiose-spezifische kinetochore Faktor MOA1, unter anderem.

Insgesamt diesem Ergebnisse liefern neue funktionale Einblick in die Rolle des Proteins Nrl1 in prä-mRNA-Splicing und Genomstabilität. Da Nrl1 in höheren Eukaryoten, einschließlich Menschen konserviert ist, erreicht dieser Studie weiter das Hefesystem. Der menschliche Ortholog von Nrl1, hNRDE-2, unten reguliert und mit Copy Number Aberrationen in Tumorzellen assoziiert darauf hindeutet, dass es als Tumorsuppressor wirken kann. Unsere Ergebnisse liefern somit die Grundlage für zukünftige Untersuchungen auf eine mögliche Rolle von hNRDE in der Krebstherapie.

TABLE OF CONTENTS

ABREVIATIONS

AS-TGS	TGS-induced Alternative splicing
cdc	cell division cycle genes
cdk	cyclin dependent kinase
Cen2	Chromosome centromere 2
esiRNA	endogenous siRNA
FACS	Fluorescence Activated Cell Sorting
imr	inner most repeat
MI	Meiotic division I
MII	Meiotic division II
min	minutes
MS	Mass spectrometry
NRDE-2	Nuclear RNAi defective-2
O/N	Over night
OD_F	final desired OD of a culture
OD_I	initial OD of a culture
omr	outer most repeat
PCR	Polymerase Chain Reaction
PTGS	Post transcriptional gene silencing
preC	pre culture
RNA-seq	RNA sequencing
siRNA	small interfering RNA
TAP	Tandem Affinity Purification
TGS	Transcriptional gene silencing
Vol_F	final desired volume
GFP	Green fluorescent protein

I INTRODUCTION

Schizosaccharomyces pombe, also called "fission yeast", is a species of yeast originally isolated in 1893 by Paul Lindner from East African millet beer and owns its name to the word for beer in Swahili. It is also a well-known model organism for molecular and cell biology, first used to study genetics and cell cycle in 1950s (1)

I.1 Cell Cycle

S. pombe is a rod-shaped cell, approximately 3µm in diameter that grows by elongation at the ends and divide by the formation of a septum that cleaves the cell at its midpoint (medial fission). The generation time is quite fast ranging between 2-4 hours, depending of media type, temperature and presence of gene defects. *S. pombe* mitotic cell cycle (**Figure 1**) has a particularly long G2 (exponential phase), which account for 70% of the division time. The remaining 30% of division time is roughly equally distributed between, G1, (DNA replication) and M phases (Mitosis) each taking about 10% of the division time. The control of the cell cycle is mediated by regulating the G2–M phase transition. Since *S. pombe* is a haploid cell and highly vulnerable to DNA damage, having a spare copy of the genome present through as much of the cell cycle as possible represents an important fail-safe mechanism and huge life advantage (2).

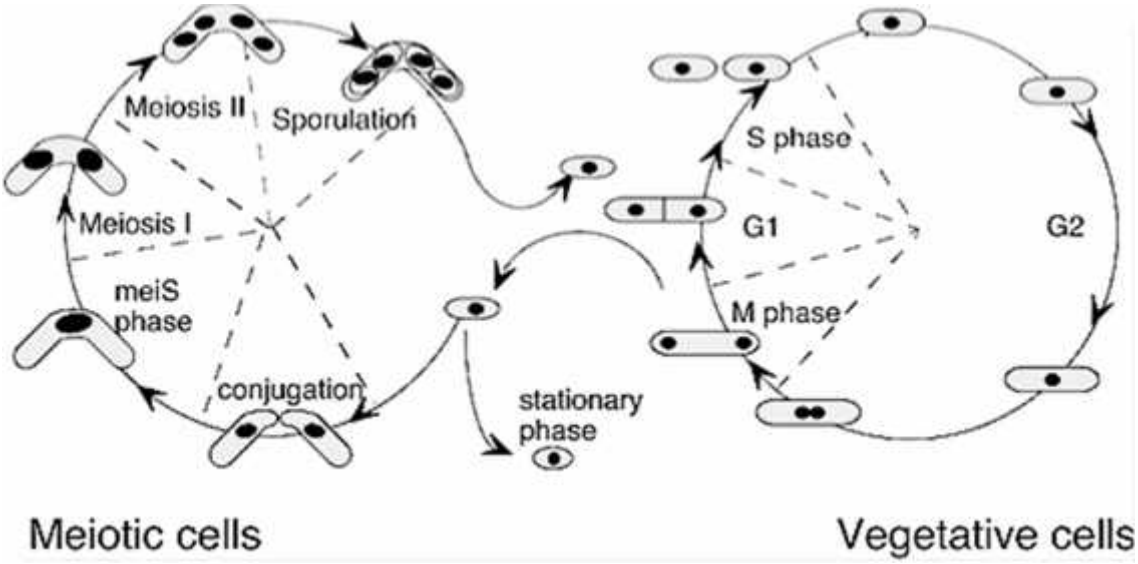

Figure 1: *S. pombe* cell cycle. Cell Cycle of Schizosaccharomyces pombe during Meiosis (left) and Mitosis (right). Taken from http://www-bcf.usc.edu/~forsburg/main4.html

The Meiotic cell cycle is specialized and occurs in response to nutrient limitation, and the presence of cells of opposite mating types. Upon starvation conjugation takes place and a transient diploid or zygote is formed. Soon after, during meiotic S phase (meiS phase) and prior to the two subsequent meiotic divisions (Mei I and Mei II) an important process in fission yeast take place, the recombination between the homologous chromosomes (**Figure 2**) a process that creates new chromosome combinations or outcomes with different alleles of each gene. The end product of Meiosis results in four spores packaged into a tetrad ascus with two distinctive characteristics compared with the starting diploid: first, they have reduced the total amount of genetic information to just one copy per cell, and second, the process of recombination within and between chromosomes resulted in four meiotic nucleus containing different genetic information. Although fission yeast is generally haploid, with a transient diploid stage only during sexual differentiation, in the laboratory, diploids can be recovered and grown in the vegetative cycle maintaining them in rich media and/or by introducing appropriate mutations at the mating type locus so that the diploid does not begin meiosis. (2-4)

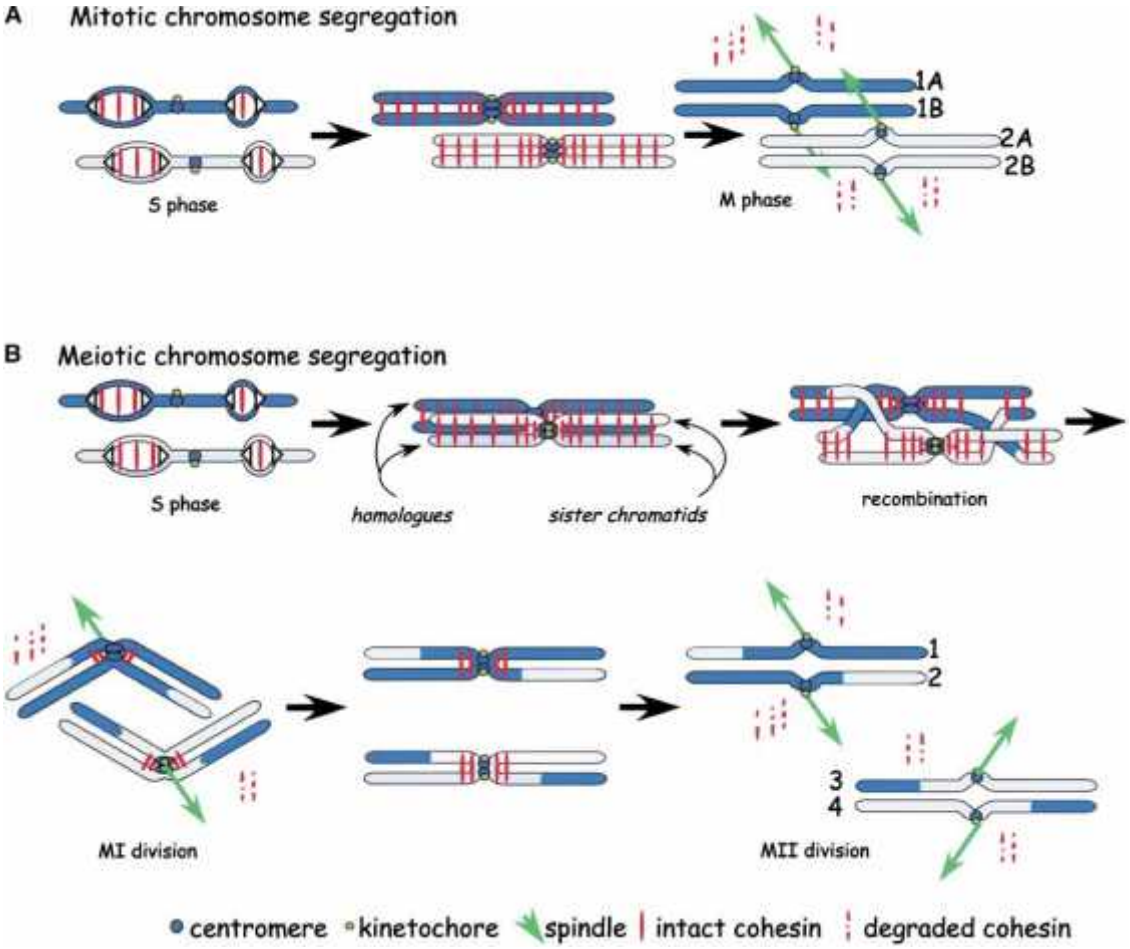

Figure 2 Chromosome events in Mitosis and Meiosis (Forsburg 2002). (A) Mitotic chromosome segregation is equational and is accompanied by loss of cohesion. Kinetochores attach to opposite spindles, and sister chromatids 1A and 2A segregate to the same daughter cell during mitosis. (B) During meiosis, recombination occurs between homologs, which are briefly held together by cohesion distal to the crossovers and by a synaptonemal complex. During MI divisions, the kinetochores are oriented to allow monopolar spindle attachment and cohesion at the centromeres is protected. The kinetochores undergo bipolar attachment in MII, and recombined homologs undergo equational division so that Chromatids 1, 2, 3, and 4 segregate to four haploid gametes.

I.2 Chromosome Structure in Fission Yeast

Fission yeast has a genome of about 12 Mb distributed in three chromosomes (**Figure 3**) of unequal length (5.6Mb, 4.5Mb and 3.5Mb respectively) with features distinctive of higher eukaryotes, including large centromeres with repetitive sequences, conserved heterochromatin proteins and epigenetic silencing mechanisms, large

replication origins, and conserved telomere proteins. Therefore, yeast has become an ideal choice to study eukaryotic chromosome structure. (5)

In 2002 the entire genome of *S. pombe* was sequenced and fifty genes with significant similarity to human disease genes were found; half of them cancer related and the rest important for eukaryotic cell organization, compartmentalization, cell-cycle control, proteolysis, protein phosphorylation and RNA splicing. In addition, the ability of fission yeast to undergo sexual differentiation and exchange genetic information makes it a very powerful model system that can provide important insights and lead the way in eukaryotic cell biology (2,5,6).

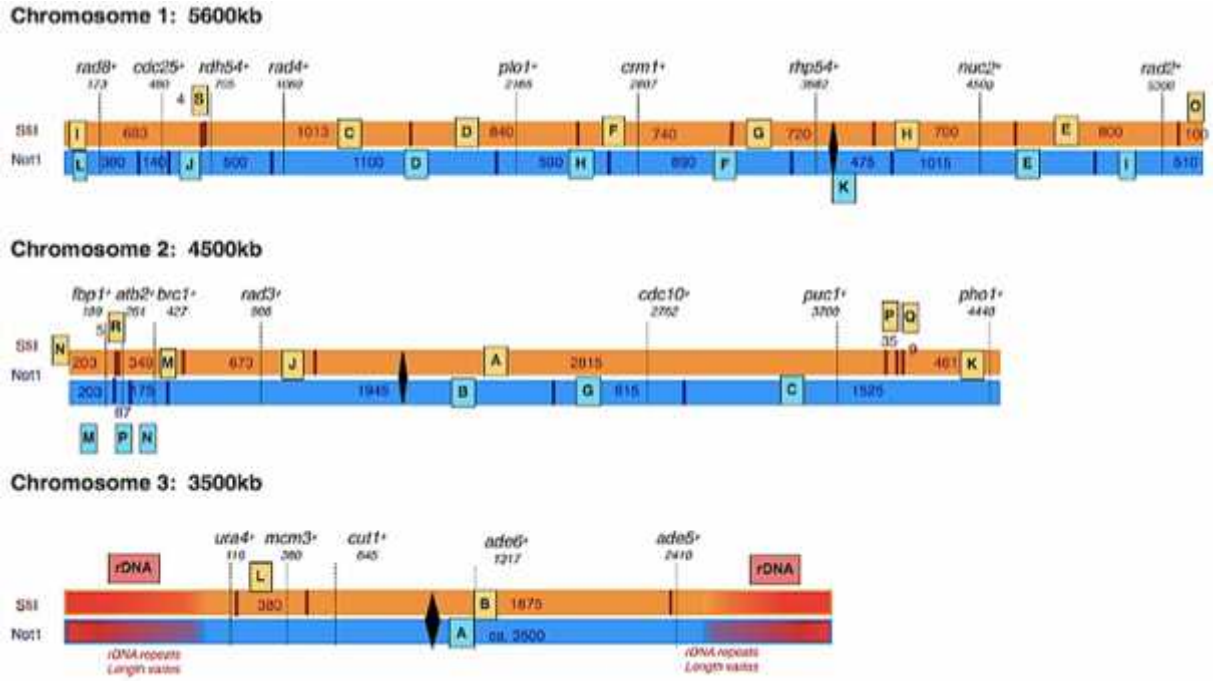

Figure 3. Schizosaccharomyces pombe Chromosome organization. Schizosaccharomyces pombe Chromosome Map taken from http://www-bcf.usc.edu/~forsburg/main7.html

I.2.1 Centromeres

Centromeres in fission yeast have a tri-partite structure composed of an inner region and two outer regions, all characterized by highly repetitive DNA (**Figure 4Error!**

Reference source not found.). The repetitive elements of the inner domain are similar to those found in the centromeres of multicellular eukaryotes making *S. pombe* a great model system for centromere research. These repetitive regions in *S. pombe* centromeres have been classified into three distinct sequence elements, the outer repeat elements (otr), the inner most repeats (imr), and the central regions (CC/cnt). The **otr** contains two different repetitive elements called dg and dh (also known as K and L, respectively), which are closely related on all three centromeres and constitute regions of constitutive heterochromatin. The chromodomain protein Swi6, homologue of the heterochromatin protein 1 (HP1) in animals, provides structural rigidity helping orient the kinetochore enabling correct association with the microtubules. The **imr** regions are imperfectly inverted repeat elements flanking the central core, different in sequence in each centromere. The **cnt** region has a specific sequence complementary for the histone H3 variant Cenp-A (Cnp1) which helps kinetochore formation and attachment of the sister chromatids (5,7,8)

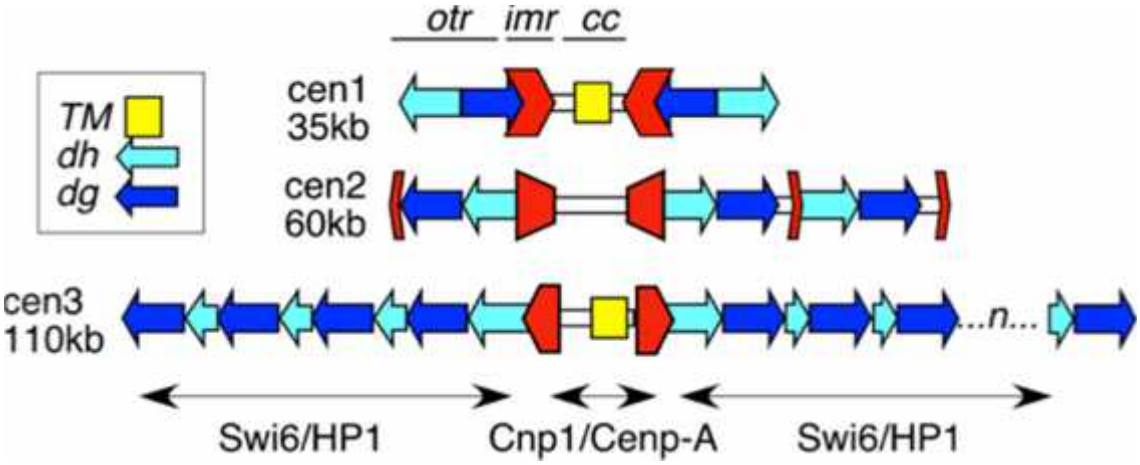

Figure 4. *S. pombe* Centromere organization. *S. pombe* centromeres showing the relative position of the otr, imr and cc repeats. CenI and CenIII have a common sequence within the central core TM, which is also found at the mating type locus. Taken from http://www-bcf.usc.edu/~forsburg/main4.html

The major heterochromatin modification at fission yeast centromeres, telomeres, mating type loci, and ribosomal DNA (rDNA) is the methylation of histone H3 at residue K9 (H3K9me), which is performed by the Clr4 methyltransferase. This last

provides a binding site for the Swi6 chromodomain resulting in chromatin condensation and silencing of the underlying sequences (5)

During each cell cycle in early S phase, the heterochromatin in the centromere domain is disassembled: H3K9me2 levels decrease and histone H3 serine-10 (H3S10) phosphorylation increases (also during mitosis) preventing Swi6–H3K9me2 binding (9). This generates a brief window for transcription of non-protein coding RNAs (ncRNA) (5). Pol II is recruited to the centromeric repeats transcribing *dg* and *dh* whose products are then rapidly cleaved or "sliced" by the RNase-H-like activity of the Argonaute Protein (Ago1). The RNA-dependent RNA polymerase Rdp1 complex (RDRC) is recruited on these transcripts and generates double stranded RNAs (dsRNA). Next, the RNase Type III Dicer processes the dsRNA into siRNA (10,11), which are loaded onto Ago1, incorporated into the RITS complex (12), containing Ago1, the chromodomain protein Chp1, and the Argonaute interacting protein Tas3. RITS helps recruit a complex containing Clr4, which methylates H3K9 enabling RITS to associate to the chromatin through Chp1 binding to H3K9me and finally promote heterochromatin assembly (5,9,13). Chp1 is then exchanged for Swi6, which can also recruit Clr4, thus initiating spreading of the heterochromatin until it reaches boundary elements (likely tRNAs) flanking the outer repeats. Therefore, heterochromatin formation in *S. pombe* is a dynamic process that occurs each time a cell enters S phase and results in heterochromatin reassembly and the re-establishment of epigenetic marks. In this dynamic process, silencing of heterochromatic regions paradoxically requires an initial phase of transcription (**Figure 5**) (9).

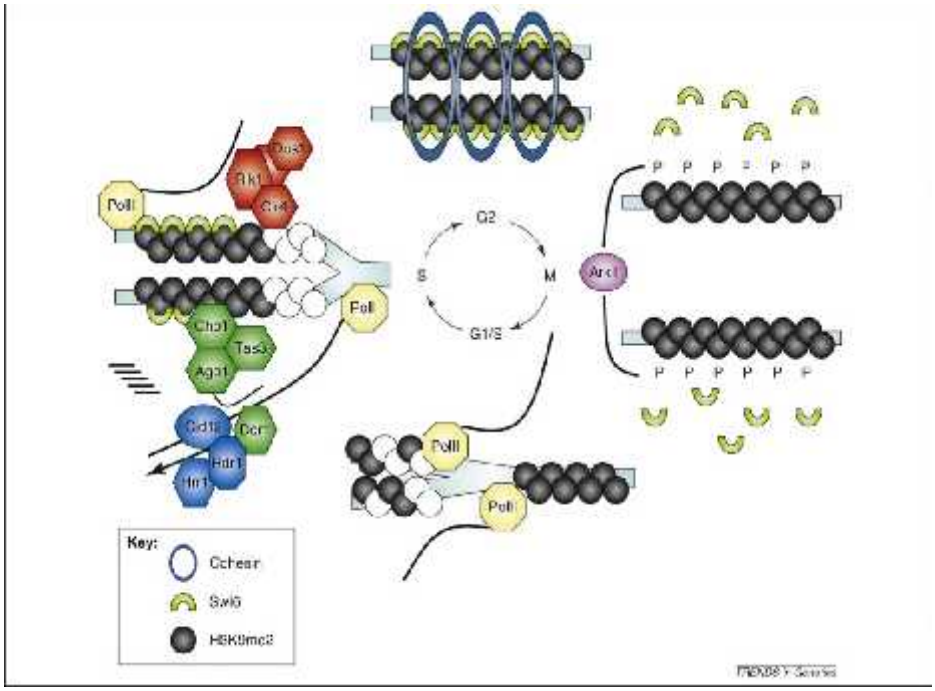

Figure 5 RNA interference (RNAi)-guided heterochromatin assembly during cell cycle. Taken from Kloc and Martienssen 2008. The Ark1 aurora kinase (purple) mediates phosphorylation of H3S10 during mitosis that leads to Swi6 (light green) ejection via the 'phospho-methyl switch'. Pericentric dh and dg repeat transcripts (black lines) appear in S phase, after replication, and are immediately processed by RNA-dependent RNA polymerase (blue) and Dicer (green) into small interfering RNAs (siRNAs). These siRNAs are then incorporated into the RNA-induced transcriptional silencing (RITS) complex (green; comprising Chp1, Tas3 and Ago1). Clr4 (red) methylates H3K9 in the G2 phase, and Swi6 is recruited back to chromatin via binding to H3K9me2. Cohesin (blue ring) is retained by Pericentric repeats through its direct interactions with Swi6 in G2. RNA polymerase II (Pol II), gold.

I.3 Mating Type switch

As mentioned before, *S. pombe* cells are normally haploid but exist two types of haploids depending their allele configuration. Heterothallic strains, which can have two possible alleles h+ and h- and therefore can only conjugate if their partner has the opposite mating type. The other type of haploid cell is known as homothallic or h90, meaning that 90% of cells are capable of switching which implicates that the strain can conjugate with itself by constantly switching its mating type from h- to h+ or viceversa inside a colony, which results in a mixture of the mating types and therefore a partner is always available (2,5)

The mating-type region on chromosome II harbors three mating-type loci: mat1, mat2P (Plus), and mat3M (Minus). The mat1 locus encodes either P or M information and is transcriptionally active while donor loci, mat2P and mat3M, are silent. The change in cell type occurs due to a replication-coupled recombination event that transfers genetic information from one of the silent-donor loci, mat2P or mat3M, into the expressed mating-type determining mat1 locus The general mechanism of the mating type switch (**Figure 6**) is by induction of a stalled replication fork during each S phase which promotes a DNA rearrangement required for cellular differentiation and in normal conditions, this event start upon nutritional starvation (14,15).

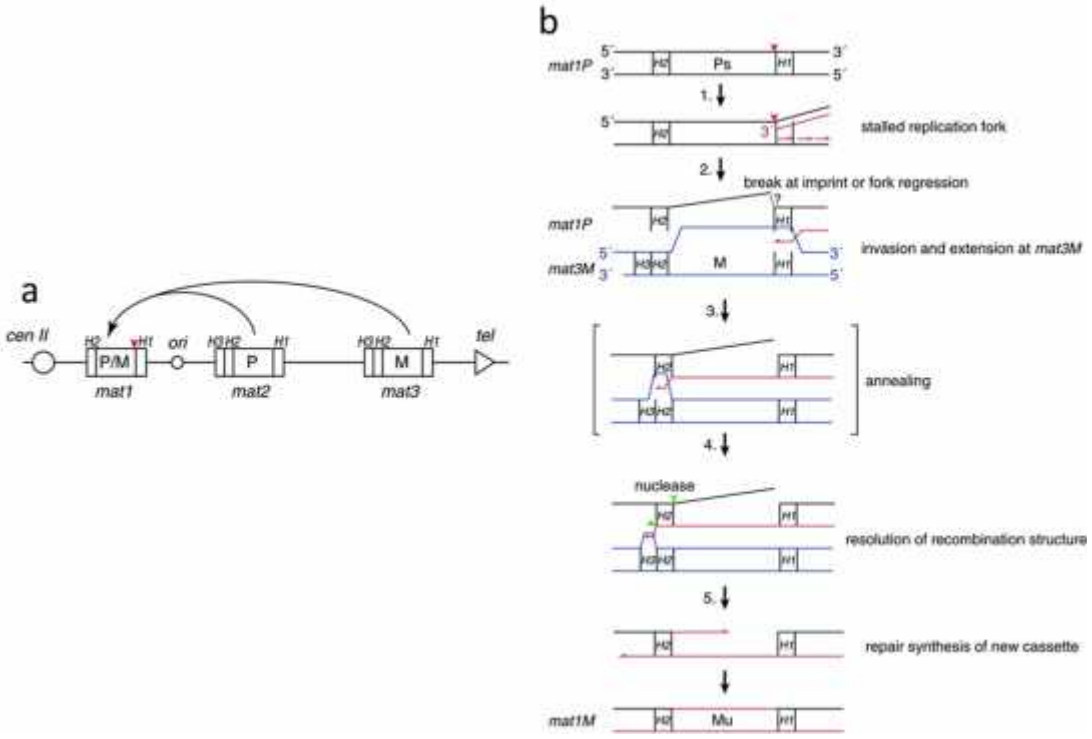

Figure 6. Scheme of mating type switch in *S. pombe* taken from Yamada et al (2007). (a) The mating-type region on chromosome II harbours the three mating-type loci: mat1, mat2Pand mat3M, where only mat 1 is transcriptionally active. Origin of replication is located between mat1 and mat2. (b). The proposed model for the underlying recombination mechanism that transfers mating-type cassette information from one of the two donor loci into the mat1 locus. (1) The replication fork (red lines) initiated at a cenII-distal origin stalls at the imprint (red arrowhead). (2) single-strand end is formed followed by a recession. The single strand invades at the homology of the H1 domain in the donor cassette and one strand of the new cassette is synthesized using the donor as template. (3) When the replication fork passes through the donor H2 domain, homology to the mat1-H2 domain is created allowing annealing between newly synthesized H2 sequence and the older mat1-H2 sequence. (4) Resolution by endonucleases leads to removal of recombination structure (green arrowheads). (5) The second strand of the new cassette is synthesized, using newly copied strand as a template and ligation leads to formation intact chromatid containing switched mat1 cassette.

I.4 RNAi in *S. pombe*

Complex organisms transcribe most of their genome, apparently in a developmentally regulated fashion and Protein-coding genes cover only a small fraction, which makes us wonder about the function of the prevalent transcription of the non-coding genome.

Noncoding RNAs (ncRNAs) are conventionally divided into short ncRNAs of 20–200 nt, also known as small RNAs (sRNA), and long ncRNAs ranging from 200 nt to 100 kb and there have been evidence that both play an important role in the regulation of gene expression (16).

There are two mechanisms by which gene expression is regulated by small double stranded RNA (sRNA). The first one occurs in the cytoplasm and is called post-transcriptional gene silencing (PTGS) and it is carried out by a phenomenon referred to as RNA interference (RNAi). The proteins that mediate RNAi, such as the Dicer like and Ago-Piwi like proteins, as well as the three major classes of sRNA - micro RNA (miRNA), small interfering RNA (siRNA) and piwi interacting (piRNA) are conserved among eukaryotes and are able to trigger degradation or translational arrest of mRNAs carrying target sequences in the cytoplasm. The second mechanism triggered by small RNAs is called transcriptional gene silencing (TGS) and, unlike PTGS, occurs in the nucleus acting directly at the gene level instead of the mRNA molecule by inducing heterochromatin formation and thus inhibiting transcription around the target site. TGS is conserved in eukaryotes, including *S. pombe, C. elegans, Arabidopsis and Drosophila,* and has also been reported to occur in mammals (17-19)

Recent evidence indicates the existence of a physical and functional link between the RNAi machinery and RNA polymerase II (Pol II) in small-RNA induced TGS.

In *S. pombe*, Pol II transcription, in addition to generating siRNA precursors, appears to play a more direct role in heterochromatin assembly (**Figure 7**) (20). Pol II

transcribes *S. pombe* centromeric repeats preferentially during S-phase of the cell cycle and this transcription is linked to targeting of the RNAi Induced Transcriptional Silencing (RITS) complex and heterochromatin assembly factors to repeat loci. Moreover, mutations in Pol II subunits impair heterochromatic assembly (21,22). Finally, heterochromatic silencing also requires splicing factors known to associate with elongating Pol II (23,24)

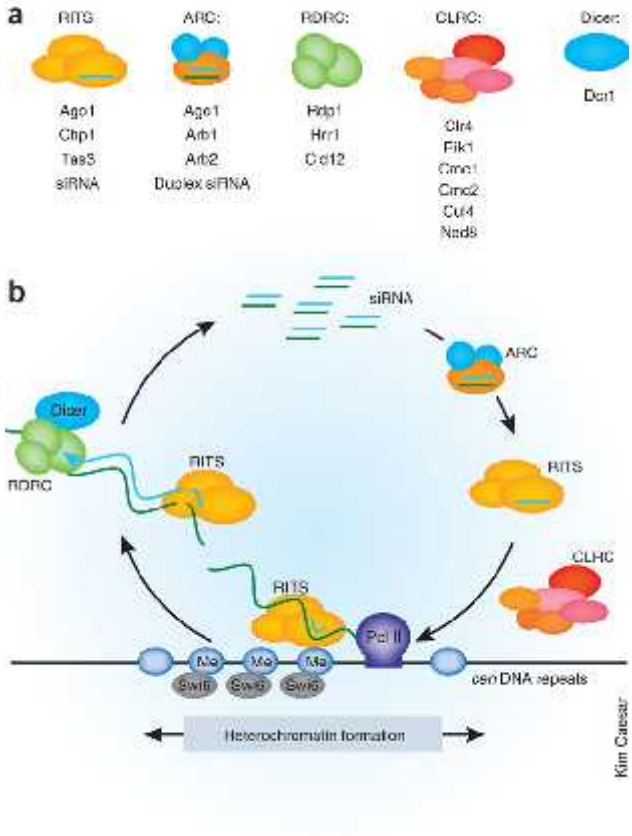

Figure 7. RNAi-mediated heterochromatin assembly in fission yeast. (a) Biochemically purified fission yeast complexes required for RNAimediated silencing. RITS, RDRC and Dicer are described in the text. ARC is an Ago1 chaperone complex that carries duplex siRNA, and the CLRC complex, which contains the Clr4 H3K9 methyltransferase, is required for H3K9 methylation and siRNA generation. (b) The nascent-transcript model proposes that the RITS complex mediates heterochromatin formation by associating with nascent transcripts via siRNA base-pairing, and with methylated H3K9 via the chromodomain of its Chp1 subunit. dsRNA synthesis and siRNA generation occur in association with specific chromosome regions and may underlie cis restriction of siRNAmediated silencing. The chromosome-associated siRNA synthesis loop is essential for the spreading of H3K9 methylation and silencing at the centromere. The coupling of the siRNA synthesis loop to H3K9 methylation forms a stable feedback loop that epigenetically maintains heterochromatin.

In the plant Arabidopsis thaliana, RNA-directed DNA elimination requires the Argonaute AGO4, the Dicer DCL3 and a plant-specific heterochromatin-dependent RNA polymerase, Pol IV (25,26).AGO4 localizes to nascent non-coding RNAs transcribed by Pol IV and recruits enzymes involved in histone H3K9 and DNA methylation.

In Drosophila RNA Pol II interacts genetically and biochemically with the small RNA silencing machinery to determine di-methylation of histone 3 on lysine 9 (H3K9me2) and deposition of the chromodomain HP1 at the chromocentric heterochromatin (27,28). In particular, PIWI is recruited to chromatin by direct association with HP1, mediated by the HP1 chromo shadow domain (CSD) and PIWI CSD-binding motif (29). The PIWI–HP1 complex may act as a RITS, in which piRNAs target nascent RNA transcribed from repeated DNA elements and tether them to chromatin.

In the nematode *Caenorhabditis elegans* and in mammalian cells recent studies have implicated TGS in the control of Pol II elongation. In *C. elegans*, a conserved nuclear protein, Nuclear RNA-interference Defective -2 (NRDE-2) has been identified to be required for RNAi and that associates with the Argonaute protein NRDE-3 and siRNAs on nascent transcripts (30). This association prevents elongation by RNA polymerase II, thereby making this a cotranscriptional form of gene silencing. The mechanism of silencing involves trimethylation of histone 3 on lysine 9 (H3K9me3) and increase of Pol II occupation at the siRNA target sites. Thus these data suggest a mechanism for nuclear RNAi: siRNA-directed co-transcriptional silencing of Pol II. NRDE-2 is therefore required for linking siRNAs to Pol II inhibition. Most interesting, NRDE-2 has single orthologues in Arabidopsis, *S. pombe*, Drosophila and human. Thus, it will be interesting to assess whether small regulatory RNAs and Pol II are similarly linked in other metazoans.

In human cells, interestingly, the phenomenon of TGS-induced alternative splicing (TGS-AS) (31) resembles that of NRDE-2 dependent TGS in *C. elegans*. In this process siRNAs targeting the intron downstream of an alternative exon promotes dimethylation and trimethylation of H3 on lysine 9 and 27, respectively. This results in

the condensation of the chromatin structure which represent a roadblock to Pol II elongation

Several studies (18,19,32) have shown that introduction of siRNAs into cancer cell lines results in transcriptional repression induction along with dimethylation of H3K9 on homologous promoters. Furthermore, endogenous siRNA (esiRNA) may represent the endogenous effector of TGS and AS-TGS have been shown to regulate gene expression in mammalian cells through histone modifications and DNA methylation (33). Finally, many naturally occurring microRNAs (miR-NAs), such as miR-134, miR-296 and miR-470, target coding sequences the genes encoding the transcription factors Nanog, Oct4 and Sox2 in mouse embryonic stem cells (34), and recent evidence indicates that human miRNAs can trigger TGS in HeLa and HEK293 cells (32).

Together, these findings lead to an apparent paradox: the physical and functional association between the RNA polymerase and heterochromatin is conserved throughout eukaryotes and mediated by the RNAi machinery. However, the role of the complex partnership between the RNAi machinery and RNA Pol II on the metazoan heterochromatin landscape remains still unexplored. The identification of the protein and RNA factors involved in this process holds promises to shed some light on this intriguing paradox of nature.

I.5 RNA polymerase II transcription and its regulation

The interaction between RNAi pathways and Pol II transcription is conserved among eukaryotes (see above). In *C. elegans* the NRDE-2 protein links RNAi and Pol II regulation: it associates to ncRNAs and mediates inhibition of Pol II elongation (30)

The *S. pombe* RNA Pol II is composed of 12 subunits, Rpb1 to Rpb12, similar to what has been described for the budding yeast S. cerevisiae (**Figure 8**) and mammalian cells (35). In particular, the Pol II subunits Rpb7, Rpb2, and Rpb1 have been shown to be required for pre-siRNA synthesis, generation of siRNA, and chromatin modifications

respectively (21,22). The large subunit, Rbp1, contains the active site and is responsible for regulation of transcription initiation and elongation through the modification of its carboxy-terminal domain (Pol II CTD) (36). This domain is composed of highly conserved repeats of a heptapeptide sequence Y1-S2-P3-T4-S5-P6-S7 (37,38). All residues within the CTD heptad repeat can be modified either by phosphorylation (tyrosine, threonine, serine) or isomerization (proline) (36). Serine 5 and serine 2 phosphorylation (Ser5-P and Ser2-P) are well studied and are conserved general marks of transcription (39) and more Importantly, correlate with different steps of the transcription cycle

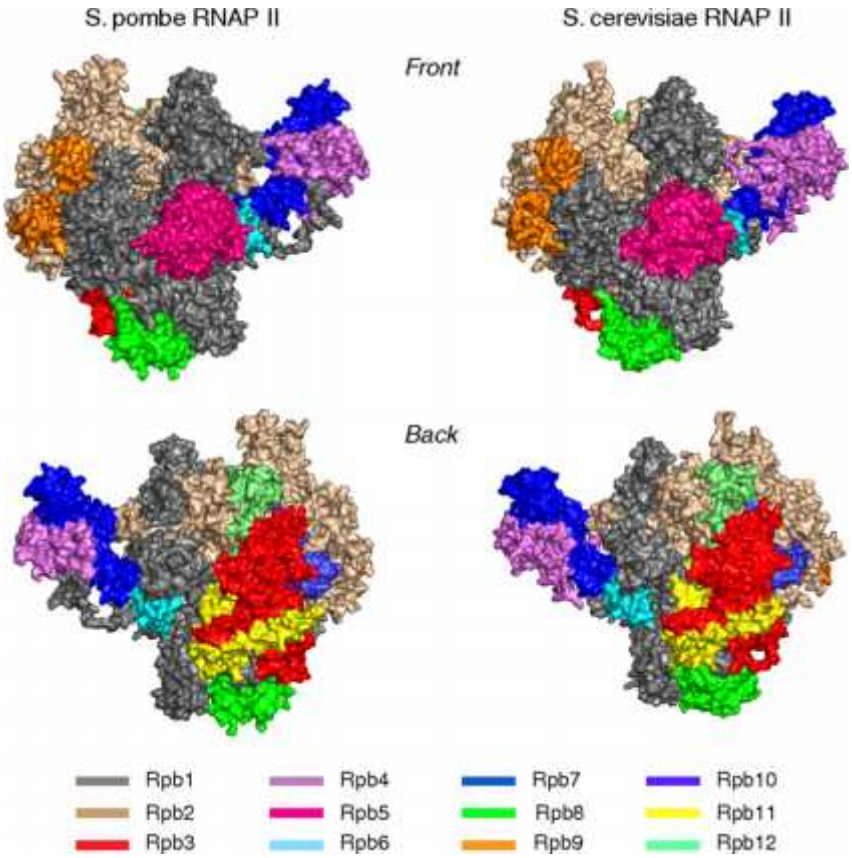

Figure 8 RNA pol II Structure. Left from *S. pombe* and right from S. cerevisiae. Surface representation of front (Upper) and back (Lower) views shown. Individual subunits are colored as indicated. Taken from Spåhr et al (40)

Ser5 phosphorylation is directly related with transcription initiation and induce the 5' end capping of nascent RNAs by helping recruit the enzymes that add a methylguanosine cap (Cap enzymes) and therefore associated with Pol II occupancy at the promoter site of the gene (41). Ser2 phosphorylation has the tightest association

with transcription elongation regulation (**Figure 9**) and it is observed as Pol II transit downstream of the Transcription Start Site (TSS) through the gene (41,42)

Ser7 phosphorylation can be found throughout gene sequence in yeast (43).However, despite its presence on protein-coding genes, its phosphorylated form is particularly important for proper transcription of snRNA genes and may or may not be required for transcription or processing of mRNA genes (44)

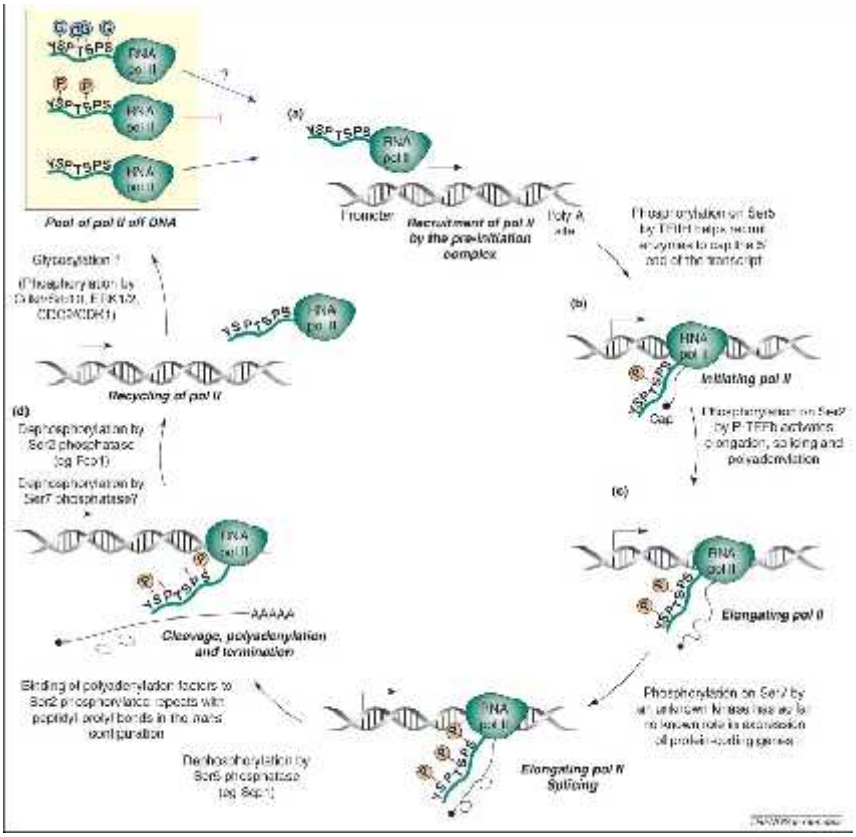

Figure 9 Modification of the polymerase II (Pol II) carboxyl-terminal domain (CTD) heptapeptide during transcription of protein-coding genes. (a) The CTD of pol II, which is recruited by preinitiation complexes at the promoter, is unphosphorylated. b) Phosphorylation of Ser5 just after initiation, helps recruit and activate enzymes that add a methylguanosine cap (filled black circle) to the 5′ end of emerging transcript. (c) Subsequent phosphorylation of Ser2 activates elongation and RNA processing. (d) After cleavage and polyadenylation of the 3′ end of the pre-mRNA, directed by the poly(A) site, dephosphorylation of the CTD may help pol II to disengage ready for another round of transcription. Glycosylation is indicated by circles containing Gs (light blue), phosphorylation by circles containing Ps (orange), and trans-isomerization of prolines by a t (red) above the amino acid. Only one heptapeptide of the multiple heptapeptide repeats is shown on the schematic of pol II (green) with a CTD 'tail. Taken from Egloff and Murphy 2008

I.6 Aim and significance of the project

Recently, orthologues of *C. elegans* NRDE-2 in *S. pombe* (SPO_C20F10), Arabidopsis thaliana (ATH_A13g17) and human (HAS_C14orf) were identified by in silico analysis (45) and their similarities were calculated: NRDE-2-HAS_C14orf 18.6%, identity and 33.7% similarity; NRDE-2- SPO_C20F10, 15.5% identity and 27.2% similarity; NRDE-2-ATH_A13g17, 15.2% identity and 29.5% similarity (**Figure 10**). The *S. pombe* NRde-2 Like protein is a 113.2 kDa nuclear protein of 972 amino acids and was named "Nrl1" and was registered on *S. pombe* gene database (http://old.genedb.org/genedb/pombe/).

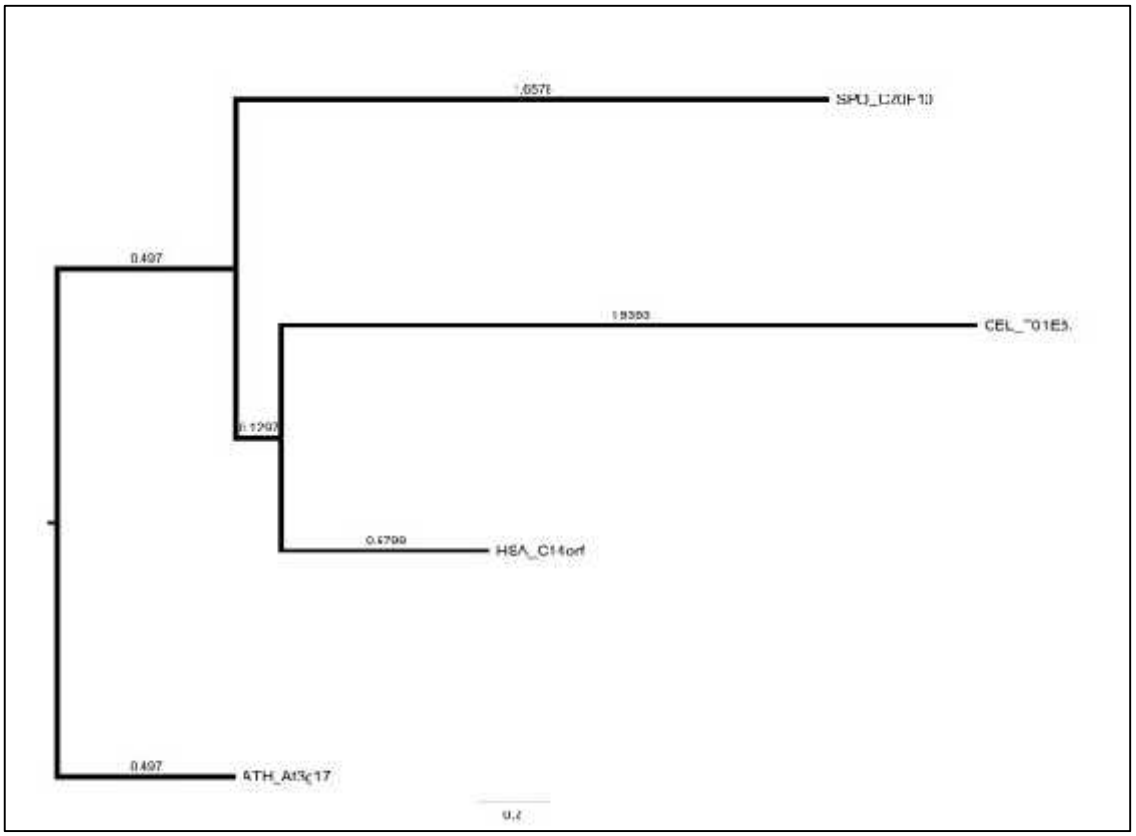

Figure 10. NRDE-2 Orthologues in *C. elegans*, *S. pombe*, Arabidopsis thaliana and Human Phylogenetic tree of *C. elegans* NRDE-2 (CEL_TO1E8) and its orthologues in *S. pombe* (SPO_C20F10), Arabidopsis thaliana (ATH_A13g17) and human (HAS_C14orf). In a global alignment the similarities are as follows (using default parameterization: BLOSUM62, gap open: 10, gap extension: 0.5): NRDE-2-HAS_C14orf 18.6%, identity and 33.7% similarity; NRDE-2SPO_C20F10, 15.5% identity and 27.2% similarity; NRDE-2-ATH_A13g17, 15.2% identity and 29.5% similarity. Taken from

An increase in mutations rates and chromosomal aberrations represent a form of genome instability and are a hallmark of most tumor cells and in addition, they are the key to development, progression and prognosis of cancer (46). Additionally, genome instability has been related to the malfunction of the DNA repair mechanisms (47), but interestingly, it has come to light that defects in mRNA biogenesis may also induce an unstable genome through the formation of mutagenic structures known as R-loops (48). R-loops are a three-stranded structure composed of an RNA/DNA hybrid and a displaced DNA strand which form during transcription when the nascent mRNA hybridizes to the complementary DNA template (48,49). Splicing, which involves the initial processing of the mRNA by the removal of a gene's introns, has been demonstrated to be a key process in the maintenance of the genome (50), and its disruption may lead to various cancer types (51). New evidence suggests that coordinated interaction of splicing factors, together with R-loop suppression and DNA repair can safeguard the stability of the genome.

The aim of the current project was to study the role of nrl1 in S. pombe and compare its activity to its orthologues in other organisms.

II MATERIALS AND METHODS

II.1 Media, Buffers and Solutions

II.1.1 Solutions

Salts x 50

52.5 g/l $MgCl_2.6H_20$	(0.26 M)
0.735 mg/l $CaCl_2.2H_20$	(4.99 mM)
50 g/l KCl	(0.67 M)
2 g/l Na_2SO4	(14.l mM)

Vitamins x 1000

1 g/l pantothenic acid	(4.20 mM)
10 g/l nicotinic acid	(8l.2 mM)
10 g/l inositol	(55.5 mM)
10 mg/l biotin	(40.8 µM)

Minerals x 10,000

5 g/l boric acid	(80.9 mM)
4 g/l MnSO	(23.7 mM)
4 g/l $ZnSO_4.7H_2O$	(13.9 mM)
2 g/l $FeCl_2.6H_2O$	(7.40 mM)
0.4 g/l molybdic acid	(2.47 mM)
1 g/l KI	(6.02 mM)
0.4 g/l $CuSO_4.5H_2O$	(1.60 mM)
10 g/l citric acid	(47.6 mM)

After autoclaving, a few drops

of preservative is added. (1:1:2,)

chlorobenzene: dichloroethane: chlorobutane)

TES: for Total RNA isolation

Tris pH 7.5	(10mM)
EDTA pH 8	(10mM)
SDS	(0.5%)

DAPI mounting media

Glycerol	(50%)
DAPI	(1µg/ml)
Paraphenyl diamine	(0.1mg/ml)
Tris pH 8	(0.1M)

II.1.2 Media and growth conditions

II.1.2.1 Growth conditions

The strains were grown at 30°C in standard yeast extract with supplements (YE6S), minimal medium (EMM), or Pombe Minimal Glutamate (PMG). For meiotic segregation assay, crosses were performed at 25°C in sporulating media (PMG-N) in order to induce meiosis upon starvation using strains with an inserted GFP marker in the chromosome 2 centromere (cen2-GFP). After generation of the tetrad ascus, cells were stained with DAPI (50% glycerol, 1µg/ml DAPI, 0.1mg/ml paraphenyl diamine and 0.1M Tris pH 8

For desired OD calculation, the following formula was used:

$$\text{preC (ml)} = \frac{(Vol_F * OD_F)/2^n}{\text{preC } OD_i} \qquad n = \frac{(\text{incubation time})}{\text{gen time}} - 1$$

preC is the pre-culture from which the initial OD (**OD_i**)was measured. **Vol_F** represents the desired final volume and **OD_F** the desired final OD of the culture. **n** represents the

total number of generations and is calculated dividing the total incubation time (hours) by the generation time of the strain (hours) minus one.

Table 1. *S.pombe* generation time according to media and temperature

Medium	Temperature (C°)	Generation time
YE	25	3h
	29	2h 30min
	32	2h 10min
	35.5	2h
Minimal	25	4h
	29	3h
	32	2h 30min
	35.5	2h 20min

II.1.2.2 Media used

Lysogenic Broth (LB)

10g Bacto-tryptone	(1% w/v)
5g yeast extract.	(0.5% w/v)
10g NaCl.	(171mM)

Edinburgh Minimal Medium (EMM 2) (Used for vegetative growth)

3 g/l potassium hydrogen phthallate	(14.7mM)
2.2 g/l Na_2HPO_4	(15.5 mM)
5 g/l NH_4Cl	(93.5 mM)
2% (w/v) glucose	(111 mM)
20 ml/l salts	(stock x 50)
1 ml/l vitamins	(stock x 1000)
0.1 ml/l minerals	(stock x 10,000)

Minimal supplemented (Used for vegetative growth)

EMM2 + 225 mg/l supplements as required.

Minimal sorbitol (EMMS - Used to grow up transformants)

As EMM. Add sorbitol to final 1.2M.

Yeast extract + supplements (YE6S - Vegetative growth)

YE+225 mg/l adenine, histidine, leucine, uracil and lysine hydrochloride.

MALT extract agar (M.E.A.)

17g of Difco Malt Extract	(1.7 % w/v)
3g Peptone	(0.3 % w/v)

Pombe Glutamate media (PMG)

3 g/l potassium hydrogen phthallate	(14.7mM)
2.2 g/l Na2HPO4	(15.5 mM)
3.75 g/l L-glutamic acid, monosodium salt (Sigma G-5889)	
20 g/l glucose	(2% w/v)
Salts	(20 ml/l)
Vitamins	(1 ml/l)
Minerals	(0.1ml/l)

Solid media was made by adding 2% Difco Bacto Agar. All media were prepared in bulk, sterilized by autoclaving at 10 psi for 20 min. Media is left to cool down in 500 ml bottles and then poured in agar plates

II.1.3 Buffers

Lysis Buffer

Triton X-100	(2% w/v)

SDS	(1% w/v)
NaCl	(100mM)
Tris-HCl pH 8.0	(10mM)
EDTA	(1mM)

SDS Buffer (Laemmli Buffer)

2.5mL Tris HCl pH 6.8

2 mL 100% Glycerol

4mL SDS 10% (w/v)

0.5mL 0.1% Bromophenol blue

H_2O up to 10mL

B-Mercaptoethanol	(2.5-5%)

LiAc

250µl 0.5M EDTA	(1.25µM)
1ml 1M Tris-HCl	(10mM)
1.02g LiAc	(0.1M)

PMSF

0.84g 100mM PMSF	(36mM)

48.2mL Isopropanol

PBST

IPP150 Buffer (500mL)

25mL 1M Tris HCl pH 8	(50mM)
15mL 5M NaCl	(150mM)
100mL 50% glycerol	(10%)
5mL PMSF (in isopropanol)	(1mM)

H_2O up to 500mL

IPP150 Lysis Buffer (300mL)

5 tablets of EDTA free PI cocktail	
6mL 1M NaF	(20mM)
15mL 0.1M Na-pyrophosphate	(5mM)
3mL 1M B-glycerolphosphate	(30mM)
1.5mL 0.2M Na3VO4	(1mM)

IPP150 Washing Buffer (200mL)

3ml 100mM PMSF (in isopropanol)	(15mM)

TEV Cleavage buffer (50mL)

0.5mL 1M Tris HCl pH 8	(10mM)
1.5mL 5M NaCl	(150mM)
50uL 0.5M EDTA	(500µM)
10mL 50% glycerol	(10%)
0.5mL 10% NP40	(0.1%)
50uL 1M DTT	(1mM)
0.5mL 100mM PMSF	(1mM)
H_2O up to 50mL	

Calmodulin Binding Buffer 1 (CBB1 50mL)

0.5mL 1M Tris HCl pH 8	(10mM)
1.5mL 5M NaCl	(150mM)
50µL 1M Mg Acetate	(1mM)
100µL 0.5M Imidazole	1mM)
100µL 1M $CaCl_2$	(2mM)
10mL 50% glycerol	(10%)
0.5mL 10% NP40	(0.1%)

35µL B-Mercaptoethanol

H2O up to 50mL

Calmodulin Binding Buffer 2 (CBB2 50mL)

0.5mL 1M Tris HCl pH 8	(10mM)
1.5mL 5M NaCl	(150mM)
50µL 1M Mg Acetate	(1mM)
100µL 1M $CaCl_2$	(2mM)
3.5µL B-Mercaptoethanol	
H_2O up to 50mL	

Calmodulin Elution Buffer (CEB 10mL)

0.1mL 1M Tris HCl pH 8	(10mM)
0.3mL 5M NaCl	(150mM)
10µL 1M Mg Acetate	(1mM)
200µL 0.1M EGTA	(2mM)
0.7µL B-Mercaptoethanol	

II.2 *S.pombe* Storage

II.2.1 Generation of Glycerol Stocks for Long Term Storage

Cells were grown in 0.8ml Yeast extract Media (YES) at 32°C for 2 days then mixed with 0.8 ml of YES containing 50% glycerol in a cryotube and cultures were placed -70°C.

II.2.2 Shorter Term Storage

Cells were kept on Agar plates with Yeast media for a maximum of 2 months.

II.2.3 Re-isolation of Frozen Cultures

Small amount of frozen glycerol stock Strain stored at -70°C was scraped off with a sterile spatula and patched onto a YES plate and incubated at 32°C for 1-4 days. After growth was visible, single colonies were streak out on YES and incubated at 32°C for 2-3 days. Strains stored on YES agar plates were directly streak out onto, and incubated at 32°C for 2-3 days. Phenotype of strains was checked prior to carrying out genetic or molecular procedures

II.3 Strains and materials for molecular biology

II.3.1 Strains

Table 2. List of strains used in this project

Name	Genotype
12618	h90 ade6-216 leu1-32 lys1-131 ura4-D18 cen2(D107)[:: kanr-ura4+-lacOp] his7+::lacI-GFP rec11::CloneNat1 deletion confirmed by colony PCR
12155	h- pat1-114 ade6-216
12156	h- pat1-114 ade6-210
16581	h+ nrl1::clonat ade6-210 leu1-32 ura4DS/E
16582	h- nrl1::clonat ade6-210 leu1-32 ura4DS/E
16585	h- pat1-114 nrl1::clonat ade6-210 leu32 ura4/DS. 12156 transformed with nrl1-TAP construct.
16586	h- pat1-114 nrl1::clonat ade6-216 leu32 ura4/DS nrl1-TAP
16587	h+ nrl1::clonat cen2-GFP. 1225 transformed with nrl1KO construct
16588	h- nrl1::clonat cen2-GFP. 1226 transformed with nrl1KO construct
16874	h90 nrl1::clonat ade6-216 leu1-32 lys1-131 ura4-D18 cen2(D107)[:: kanr-ura4+-lacOp] his7+::lacI-GFP. Transformed with nrl1ko plasmid
16927	h-/h- pat1-114/pat1-114 ade6-M210/ade6-M216 nrl1-TAP::KanMX6/nrl1-TAP::KanMX6 created by protoplast fusion
17100	h+ swi6::KanMX imR(NcoI)::ura4oriI leu1-32 ade6- hi3-D1? ura4-DS/E
17106	h+ nrl1-TAP::kanMX6 ade6-M210 his7 lys1 leu1 ura4

II.3.2 DNA Oligonucleotides

Table 3. DNA Oligonucleotides used for PCR for checking positive transformants of Nrl1Δ strains

Oligo Name	Sequence
Nrl1KO upch	GAGAAGCGGGCTGTTTTTCG
upch-uni	GTCGTTAGAACGCGGCTACA
Nrl1KO dwch	CCACATTAAACTGCCACCGC
dwch-uni	TCTGGGCCTCCATGTCGCTGG
nrl1WT1_Fw	AGAAACCCCAAGTGAAGTAAGT
nrl1WT1_Rv	CTTCCTTGCTGGCGCAATTT
nrl1WT2_Fw	TGGCATGGCTTCCAGTGAAT
nrl1WT2_Rv	ACATCTACTTACTTCACTTGGGGTT

II.3.3 Cloning Vector

pnko1, namely pCloneNat1 K4421 vector (**Figure 11**) including the deletion construct for Nrl1, was derived from Kim Nasmyth DNA collection and includes selective markers for ampicillin resistance and the natMX4 cassette which confers resistance to nourseothricin. In addition has sequences specific for several restriction enzymes respect both markers are (52).

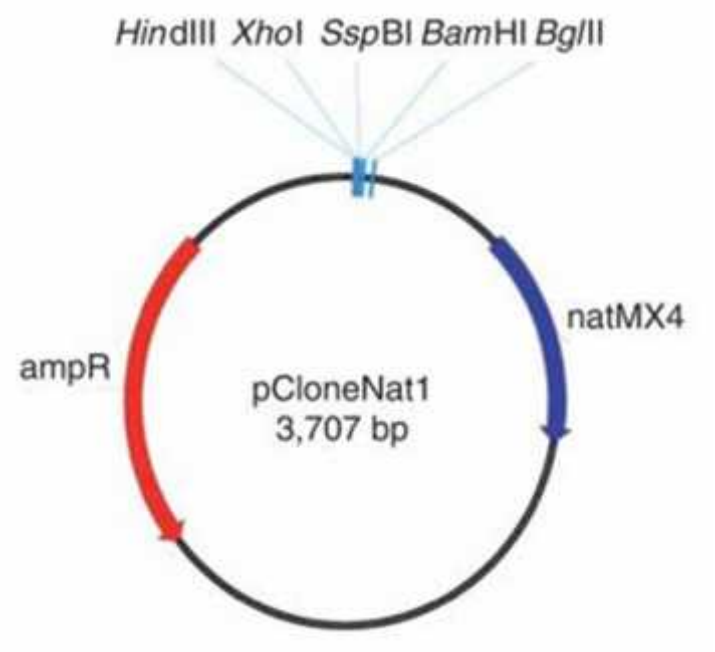

Figure 11 pCloneNat1 Vector map. pCloneNat1 K4421 vector map (derived from Kim Nasmyth DNA collection)

II.3.4 Antibodies

Table 4. List of antibodies used

Antibody Name	Producer
Rabbit Anti Phospho RNA Polymerase II (S2)	Behyl A300-654A
Phospho RNA Polymerase II (S5)	Bethyl A300-655A
Rat Anti-RNA polymerase II subunit B1 (phospho-CTD Ser-7	Sigma clone 4E12
PAP, Rabbit polyclonal	Dako Z0113
anti pol II	Santa cruz sc-56767
Anti-β-Actin−Peroxidase	Sigma A3854
Affinity purified Anti Spt5	(Schwer, 2009)

II.4 Methods

II.4.1 Image Collection

Cells were observed using a Delta Vision Core wide field deconvolution microscope (Applied Precision, Issaquah, WA, USA) using an Olympus 603/1.40, PlanApo, NA = 1.40 objective lens and a 12-bit Photometrics CoolSnap HQII CCD, deep-cooled, Sony ICX-285 chip. The system x-y pixel size is 0.1092 mm x-y. softWoRx v4.1 (Applied Precision) software was used at acquisition electronic gain = 1.0 and pixel binning131. Excitation illumination was from a solid-state illuminator (seven-color version); DAPI was detected with a 0.2-s exposure. Suitable polychromic mirror Sem-rock DAPI/FITC/A594/Cy5 API#52–852112–000 bs generally: 433/55–522/34–593/64–655LPish was used.

II.4.2 Chromosomal DNA Isolation of *S. pombe*

S. pombe cells were culture in 2mL YES and incubated at 32°C Overnight (O/N). Cells were harvested by centrifugation at 4500 rpm for 1min and re-suspended in 0.5ml of ddH_2O in 1.5ml Eppendorf tubes. Cells were centrifuged at 16,000 rpm for 5 seconds and supernatant was discarded. Pellet was then re-suspended with 0.2ml of Lysis Buffer in 2mL screw-cap cryotubes and 0.2ml Phenol: Chloroform (25:24:1) was added, along with acid pre-washed glass beads. VWR Digital Disruptor Genie cell disruptor was used at 4°C and broken cells were transferred to 1.5ml Eppendorf tubes. Cells were centrifuged at 14,000 rpm and 150 µl of supernatant was collected and transferred into a new 1.5ml Eppendorf tube. 1/10 vol (15µl) of 3M NaOAc pH 5.2 was added along with 2.5 vol (375µl) of pre-chilled (-20°C) Ethanol 100%. Cells were centrifuged at 14,000 rpm and washed two times with 70% Ethanol (-20°C). Supernatant was then discarded and precipitated DNA was air-dried in an Eppendorf ThermoStat. Dried cells pellet was re-suspended in 200 µl of 1X TE buffer (10 mM Tris-HCl pH7.5, 1mM EDTA including 1µl RNase A 10mg/ml) and then incubated at 37°C for 30 min. Resulting DNA was then checked by Electrophoresis in 1% Agarose Gel.

II.4.3 Transformation of *S. pombe*

II.4.3.1 Design of deletion Construct

Gregan and col (2006) designed a knock out strategy to delete genes in *S. pombe* (**Figure 12**), based on knockout constructs containing homologous regions to the target gene that were cloned into pCloneNat1 vector K4421 (53), which includes a dominant drug- resistant marker. In this way, primers were designed distal ("upout" and "dwout") to nrl1 gene containing 5'-tails encoding a restriction site for XbaI. The proximal primers ("upin" and "dwin") were designed to contain 5'-tails encoding restrictions site for XhoI (upstream) and BglII (downstream). After amplification by PCR, products were mixed and purified and the ligated using T4 ligase (Invitrogen). Products were digested with XhoI and BglII to create sticky ends and since the products are of unequal size, after separation in Agarose gel, 5 bands should be seen. The desired heterodimer band is then is excised from the gel and DNA is extracted using a column. The purified heterodimer is ligated to pCloneNat1 previously digested with XhoI and BglII and bacteria are transformed. The resulted positive construct was named pnko1

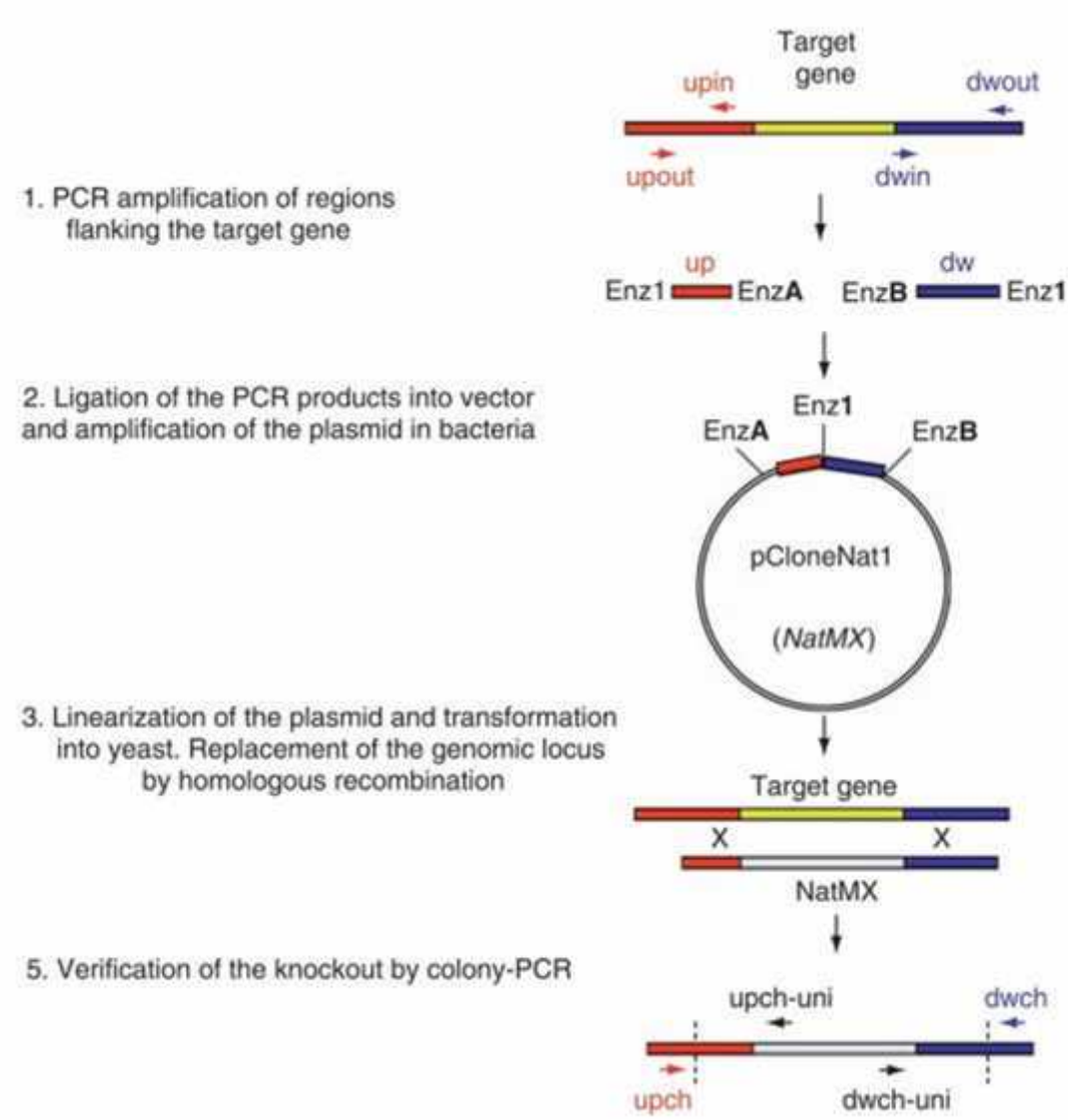

Figure 12 Nrl1Deletion construct diagram. Taken from Gregan et al (2006). Flowchart of the knockout strategy. Regions flanking the target gene upstream of the start codon and downstream of the stop codon are designated as “up” and “dw”, respectively. PCR primers were designed in silico so that 150–700 bp of up and dw regions are amplified. Combination of primers upout + upin and primers dwout + dwin is used to PCR amplify regions upstream and downstream of the target gene, respectively. These are the homology regions used to knock out the target gene. Primers encode restriction sites, which are used to clone the homology regions into the pCloneNat1 vector. The vector containing homology regions is linearized (linearization in the homology region increases efficiency of the targeting) and transformed into yeast. Homologous recombination is used to replace the target gene with the knockout construct. The knockout is verified in yeast transformants by colony PCR using combination of primers upch and upch-uni and primers dwch and dwch-uni.

II.4.3.2 Plasmid Miniprep

E. coli bacteria containing the pnko1 plasmid was grown in LB media with ampicillin (100mg/ml)at 37°C overnight and plasmid purification was carried out using the PureYield™ Plasmid Midiprep System (Promega A2495)

II.4.3.3 Preparation of competent cells for transformation

S. pombe yeast strain was grown in 3 ml YE6S in 250 ml Erlenmeyer at 32°C O/N, then 3 ml of culture were inoculated in 15mL Falcon tube at OD595=0.2 and grown for 4-5 h at 32°C until an OD_{595}=0.6. 1,5 mL of culture was centrifuged for 2min at 5000 rpm, supernatant was discarded and cells were washed twice with 1 ml LiAc solution (0.1 M LiAc in 1x TE, pH=7.5) for 3min at 5000 rpm and finally re-suspended in 150 µl LiAc solution and incubated in an Eppendorf thermomixer for 30min at 32°C and 750 rpm.

II.4.3.4 Transformation

After preparing 1mL competent cell suspension, 10µL of pnko1 vector (derived from pCloneNAT1 plasmid containing *natMX4* maker gene (CloNAT resistant) was added in addition to 2µL of Sperm Salmon ssDNA and 375 µl PEG solution (PEG 40% diluted with LiAc 0,1M pre warmed at 32°C) and then mixed. Sample was then incubated in an Eppendorf® Thermomixer® at 32°C for 55 min and then summited to heat shock (46°C for 5 min). Sample was then washed twice for 1min at 5000 rpm and pellet was re-suspended and then inoculated to a final 1mL of Yeast extract Media and incubated O/N at 32°C with shaking at 200 rpm. 50 µL of culture were inoculated in selective plates carrying CloNAT antibiotic (100µg/mL) and incubated at 32°C for 3 days.

II.4.3.5 Check-up of Tansformants cells by PCR

Single colonies of positive transformants from selective plates carrying CloNAT antibiotic (100µg/mL) were scraped and resuspended in 50 µl of H_2O and then used as a template for the polymerase chain reaction assay using two primers specific for the

target gene ("upch" and "dwch") and two primers specific for the plasmid ("upch-uni" and "dwch-uni"). The knockout was verified by colony PCR using combination of primers upch and upch-uni and primers dwch and dwch-uni (Program 37x 50 seconds 94 °C, 60 seconds 60 °C, and 180 seconds 72 °C)

II.4.3.6 Construction of Diploid strains by Protoplast procedure

Cells were grown O/N in 10 ml of minimal medium containing 0.5% glucose and supplements to OD_{595} of 0.2-0.5, then cells were harvested at 2000rpm for 5 min and resuspended in 0.5 ml of 20mM Citrate/phosphate pH 5.6 (2.82g/l Na_2HPO_4, 4.2 g/l citric acid) and 40mM EDTA pH 8.0. Cells were then centrifuged as before and pellet was resuspended in 0.5 ml of 50 mM Citrate/ Phosphate pH 5.6 (7.1 g/l Na_2HPO_4, 11.5 g/l citric acid) and 1.2M Sorbitol. At this point, each cell suspension coming from the two strains desired to be fusion were mixed together in a ratio of 1:1 and 25 mg of NovoZymTM 234 was added and fusion tube was incubated at 37°C for 15-30 min. Spheroplasts formation was controlled under the microscope. Next, cells were washed three times with 1.2 M sorbitol, 30mM Tris-HCl pH7.6 at 2000 rpm for 15 sec. and then resuspended In 1 ml of 1.2 M sorbitol, 30mM Tris-HCl pH7.6. Then cells were centrifuged at 2000 rpm for 15 sec and resuspended in 0.3ml of 10mM Tris HCl pH 7.6, 10mM $CaCl_2$ and 30% PEG 4000. Cells were the incubated at 25°-30°C for 30 min. Finally, 0.15 ml of lower fraction was plated onto minimal sorbitol plates and incubated for 5-14 days at 29-32°C.

II.4.4 Synchronization of *S. pombe* cultures in Meiosis

To synchronize *S. pombe* cells in meiosis Diploid and haploid *pat1-114* Ade-M210 strains were used. This strains are adenine mutants whose colonies turn pink in a low adenine media (selective media for transformation) and carry a temperature-sensitive allele of the Pat1 (Ran1) protein kinase, which is a negative regulator of meiosis. *pat1-114* strains were grown in YES-Ade liquid medium to an OD_{595} = 0.5 at 25°C. The cells were collected by centrifugation, resuspended in PMG-NH_4Cl medium (supplemented with salts, vitamins and minerals) and incubated at 25°C for 16 hours to arrest cells in

G_1. Cells were then resuspended in fresh PMG+NH_4Cl (supplemented with salts, vitamins and minerals) and induced into meiosis by shifting temperature to 34°C. To monitor the progression of meiosis, 0.5 ml of culture was fixed in 70% ethanol and then analysed by flow cytometry (54).

II.4.5 Bradford Assay

Standard curves were prepared with BSA dilutions in 0.15 M NaCl. 1 mL of Bradford dye (AppliChem) was added to 100 µL of protein sample. Protein concentrations were measured in an Eppendorf BioPhotometer® at 595 nm. The time between the addition of dye and the measurement were equal for every sample (55)

II.4.6 Protein purification

II.4.6.1 TCA extraction

For simple protein extraction TCA methodology was followed. 10ml cultures were grown in YPD medium to an OD_{595} of 0.4. Cells were collected by centrifugation and washed with 20% TCA. All purification steps were performed on ice with pre-chilled solutions. Cell pellets were resuspended in 250µl 20% TCA and subjected to glass bead lysis. The suspension minus the glass beads was collected, 1ml of 5% TCA was added, and precipitated proteins collected by centrifugation. Pellets were washed with 750µl 100% ethanol and proteins solubilized in 50µl 1M Tris pH8.0 / 100µl 2X SDS-PAGE loading buffer (60mM Tris pH 6.8, 2% SDS, 10% glycerol, 100mM DTT, 0.2% bromophenol blue). After 5 minutes at 95°C, insoluble material was removed by centrifugation and the supernatant analysed further.

II.4.6.2 Tandem Affinity purification (TAP)

For the Nrl1 protein purification, previously TAP tagged strains were used. This construct consist of a fusion cassette encoding CBP, a TEV cleavage site, and ProtA. The TAP method involves the fusion of the TAP tag to the target protein and the introduction of the construct into the host cell (**Figure 13**) (56). Cells expressing Nrl1-TAP were grown

in 16 L of complete yeast extract medium (YE+5S) to mid-log phase (OD ~0.8). Following, cells were harvested by centrifugation and Nrl1TAP associated proteins were isolated. Briefly, yeast cell powder was obtained using SPEX Sample Prep 6870 Freezer/Mill. Proteins were extracted using IPP150 buffer (1g of powder per 3 mL of IPP150 buffer) (IPP150, 50 mM Tris pH 8.0, 150 mM NaCl, 10% glycerol, 0.1% NP-40, supplemented with complete protease and phosphatase inhibitors and 1 mM PMSF). 500 µL of IgG beads was incubated with protein extracts for 2 h at 4°C. Beads were washed with 20 volumes of IPP150 buffer and with 5 volumes of TEV cleavage buffer (TCB, 10 mM Tris pH 8.0, 150 mM NaCl, 10% glycerol, 0.1% NP-40, 0.5 mM EDTA, 1 mM DTT). Cleavage step was performed in 2 ml of TCB buffer supplemented with 400 units of AcTEV™ protease for 2 h at 16°C. Eluate was supplemented with 6 µl of 1 M CaCl2, mixed with 6 ml of Calmodulin binding buffer 1 (CBB1, 10 mM Tris pH 8.0, 150 mM NaCl, 10% glycerol, 0.1% NP-40, 1 mM imidazole, 1 mM Mg-acetate, 2 mM CaCl2, 10 mM ß-mercaptoethanol), 200 µL of calmodulin beads and incubated for 2 h at 4°C. The beads were washed with 10 volumes of CBB1 and 5 volumes of Calmodulin binding buffer 2 (CBB2, 10 mM Tris pH 8.0, 150 mM NaCl, 1 mM Mg-Acetate, 2 mM CaCl2, 1 mM ß-mercaptoethanol). The proteins were step-eluted using 200 µL of elution buffer (10 mM Tris pH 8.0, 150 mM NaCl, 1 mM Mg-acetate, 2 mM EGTA, 1 mM ß-mercaptoethanol). Eluted proteins were separated on SDS-PAGE and visualized by silver staining. For Western blot, protein concentration was estimated by Bradford assay and after separated on SDS-PAGE, proteins were transferred to a PVDF membrane which then was incubated with PBST solution (5% milk was added) overnight at 4°C Membrane was then incubated with PAP Dako antibody (1:15,000) at 4°C for 2 hours and X-Ray film was then developed to

visualize positive isolation of the protein. Eluates from peak fractions were combined and submitted for LC-MS/MS analysis.

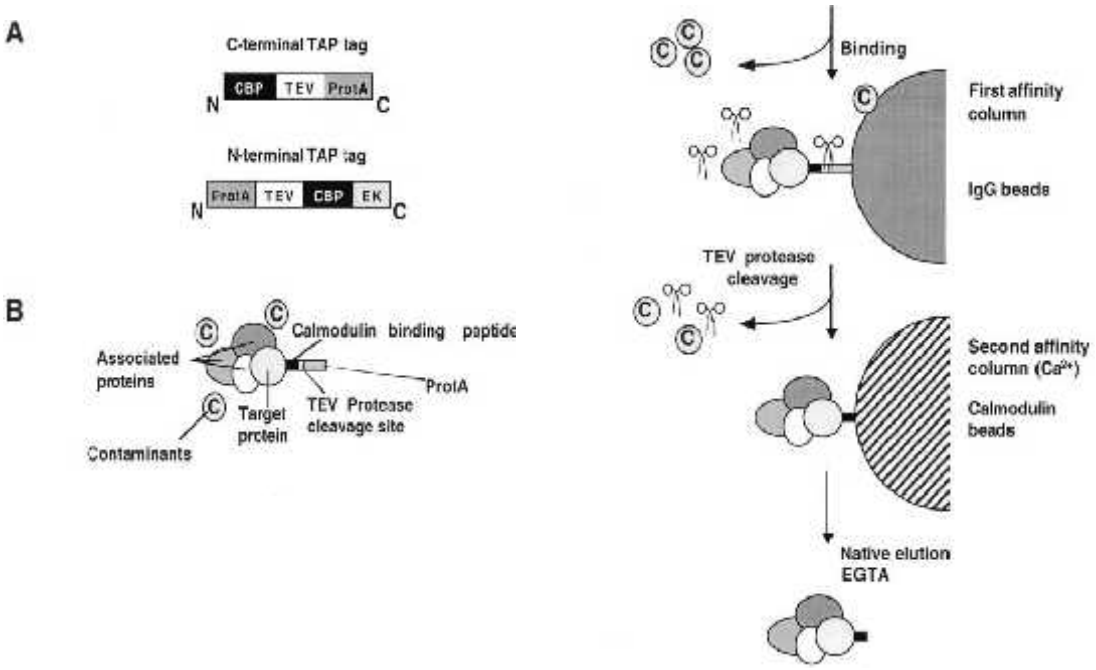

Figure 13 Tag Methodology. (A)Schematic representation of the C- and N-terminal TAP tags. (B) Overview of the TAP purification strategy.

II.4.6.3 Enzymatic digest, LC-MS/MS analysis and data analysis

The mass spectrometry analysis was carried out by the services of the Mass Spectrometry Facility at the Max F. Perutz laboratories. For this, the pH of the eluted protein sample was adjusted to 8.5, disulphide bonds were reduced with DTT and subsequently alkylated with iodoacetamide. Proteins were digested with trypsin (recombinant, proteomics grade, Roche; 1:25 of the estimated amount of protein) at 37°C overnight and stopped by addition of trifluoroacetic acid (TFA) to approx. pH 2. Digests were separated on an UltiMate 3000 RSLCnano LC system (Dionex, Thermo Fisher Scientific). Peptides were loaded onto a trapping column (PepMap C18, 5µm particle size, 300 µm i.d. x 5mm, Dionex, Thermo Fisher Scientific) equilibrated with 0.1% TFA and separated on an analytical column Acclaim PepMap RSLC C18, 50 cm × 75 µm × 2 µm, 100 Å, Dionex, Thermo Fisher Scientific) applying a 60 minutes linear gradient from

1.6% up to 30% acetonitrile (ACN). The HPLC (nano RSLC from Dionex, Thermo Fisher Scientific) was directly coupled to a QExactive mass spectrometer (Thermo Fisher Scientific) via a nanoelectrospray ionization source (Proxeon, Thermo Fisher Scientific). The electrospray voltage was set to 1900 V. The QExactive mass spectrometer was operated in the data-dependent mode: 1 full scan (m/z: 350-1650, resolution 70000) with lock mass enabled was followed by maximal 12 MS/MS scans. The lock mass was set at the signal of polydimethylcyclosiloxane at m/z 445.120025. The 12 most intense ions were fragmented by higher energy collisional dissociation (HCD) with normalized collision energy of 30. Fragment spectra were acquired with a resolution of 17500. The ion target value for full MS was set to 1,000,000, for MS/MS to 100,000. Fragmented ions were excluded from further selection for 30 s. Raw data were searched with MaxQuant 1.5 against the *S. pombe* DB (5144 entries, 2014-05-09, http://www.pombase.org/) including the contaminant collection with the following parameters: trypsin was selected as protease allowing two missed cleavages, carbamidomethylcysteine was set as static modification, oxidation of methionine, phosphorylation of serine, threonine and tyrosine as well as protein N-terminal acetylation as variable modifications. Precursor tolerance was set to 4.5 ppm and 20 ppm MS/MS for the fragment tolerance. Results were filtered at the peptide and at the protein level to 1% FDR. Relative quantification was based on the total peak intensities for each protein calculated with MaxQuant. For comparison protein intensities were normalized to the intensity of Nrl1 in proliferating cells.

II.4.7 RNA isolation and library preparation

Total RNA following Hot phenol method (57) was performed from WT and *nrl1Δ* strains, which were grown in YE6S liquid cultures at mid-exponential phase (OD_{595}= 0.2-0.4) and then harvested by centrifugation at 2000 rpm and the pellet was snap frozen in liquid nitrogen after discarding the supernatant. Cells were resuspended in 1 ml of pre-chilled DEPC water and centrifuged again at 5000 rpm and pellet was resuspended with 750 µl of TES solution and 750 µl acidic phenol-chloroform (refrigerated, Sigma P-1944).

Samples were vortexed and incubated at 65°C in a heat block for 1 hour with intervals of 10 min of vortexing. Samples were put on ice for 1 min, vortexed for 20 sec, and centrifuged for 15 min at 14,000 rpm at 4°C. 700 µl of water phase was transferred to pre-spinned (14,000 rpm at 4°C) phase-lock tubes (Eppendorf) already containing 700 µl of acidic phenol-chloroform. Samples were thoroughly mixed by inverting and centrifuged 5 min at 14,000 rpm at 4°C. 700 µl of water phase was transferred to pre-spinned (14,000 rpm at 4°C) phase-lock tubes (Eppendorf) already containing 700 µl of chloroform: isoamyl alcohol (24:1). Samples were thoroughly mixed by inverting and centrifuged 5 min at 14,000 rpm at 4°C. 500 µl of water phase was transferred to 2ml Eppendorf tube containing 1.5 ml of 100% EtOH (-20°C) and 50 µl of 3 M NaAc pH 5.2. Samples were incubated overnight at -20°C and RNA was precipitated by centrifugation for 10 min at 14,000 rpm at RT after water phase was discarded. Samples were air dried for 5 min at RT, then resuspended in 100 µl of DEPC water and incubated 1 min at 65°C. Total RNA quality was determined by Agarose 1% gel electrophoresis and concentration was estimated by spectrophotometry at $OD_{260/280}$ and then RNA was purified using Qiagen RNeasy columns. Purified RNA concentration was estimated and quality was determined by spectrophotometry and gel electrophoresis.

Strand specific cDNA libraries were prepared with lexogen SENSE protocol using poly(A)+ RNA as described (58). Two biological replicates were used for each sample and libraries were sequenced by the Illumina platform (Next generation sequencing facility of the Vienna Biocenter Core Facilities). The resulting paired end sequencing reads (100 bp long) of each sample and biological replicate were aligned independently using Tophat v2.0.11 (59). The following not default parameters were used for performing the alignment: -i 30, -I 2000, -p 16, -a 15 --library-type fr-firststrand, --b2-very-sensitive, --microexon-search and -G (gene annotation *S. pombe* ASM294v2).

The Splicing analysis was performed using the splice junctions predicted by Tophat. Only those introns that present at least two unique reads in both biological replicates were used for further analysis. Introns were classified as new if they were not

included in the gene annotation. To determine differences in intron splicing, the PSI (percentage of spliced in) was calculated by using uniquely mapped splice junction and exonic reads. Only those changes over 15% (ΔPSI > 15) and a P-value ≤ 0.05 between WT and nrl1Δ are shown. For obtaining differentially expressed genes between a pair of samples Cuffquant and Cuffdiff from the Cufflinks v2.2.1 package were used (60).

The Splicing and gene expression analysis was performed by a bioinformatician at the Department of Medical Biochemistry of the Medical University of Vienna (45)

II.4.8 Meiotic segregation analysis

Haploid heterothallic strains h- and h+ and homothallic stains h90 harbouring a GFP marker close to centromere of chromosome 2 (61) were grown on a MEA medium and incubated for 24h hours at 32°C. For analysis of meiotic segregation, homothallic strains were used, whereas for analysis during MI, only one of the heterothallic strains (h- or h+) contained a marked chromosome II (cen2-GFP) and was crossed with its opposite mating type with an unmarked chromosome II. The crosses were carried out by taking a full loop of and then mixed together (in case of heterothallic strains) and streaked horizontally on PMG-N and incubated at 25°C for 2-4 days. Colonies were then observed by microscope and segregation of marked chromosomes were examined through observation of GFP emission.

II.4.9 Statistics analysis

The non-parametrical statistical test, the Wilcoxon signed rank test, was used to evaluate the significance of the difference between WT and nrl1Δ phosphorylation levels of the RNA polII Rpb1 serine residues (Ser2, Ser5 and Ser7).

III RESULTS

III.1 Creation of *nrl1Δ* strain

In the worm *Caenorabditis elegans* the protein NRDE-2 is required for nuclear RNAi silencing by inhibition of transcription elongation (30). Thus, in order to understand the role of Nrl1, it was decided to create an *nrl1* deletion mutant (*nrl1Δ*) by replacing the *nrl1*$^{+}$gene with a *natMX4* drug resistance cassette (strain 16873). For this purpose, *S. pombe* wild type cells were transformed with pnko1 vector carrying the deletion construct (see section II.4.3 of Materials and Methods). First, pnko1 vector was linearized with XbaI and complete digestion was observed by agarose gel 1% (**Figure 14**). After choosing the best suitable plasmid, transformation of WT strain 12618 was performed as previously described (Methods). Following growth of positive transformant on selective plates (carrying ClonNAT drug), colony PCR was performed from positive clones (16874 clone nrl1ko 2,4 and 8) and then controlled by agarose gel 1% (**Figure 15**).

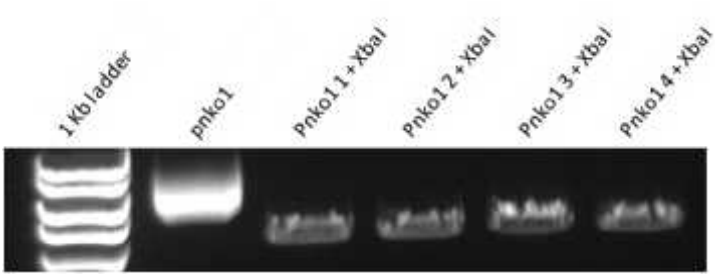

Figure 14 Linearization of pnko1 with XbaI. pnko1 was linearized using enzyme XbaI and run in agarose 2% prior transformation assay of 12618 strains

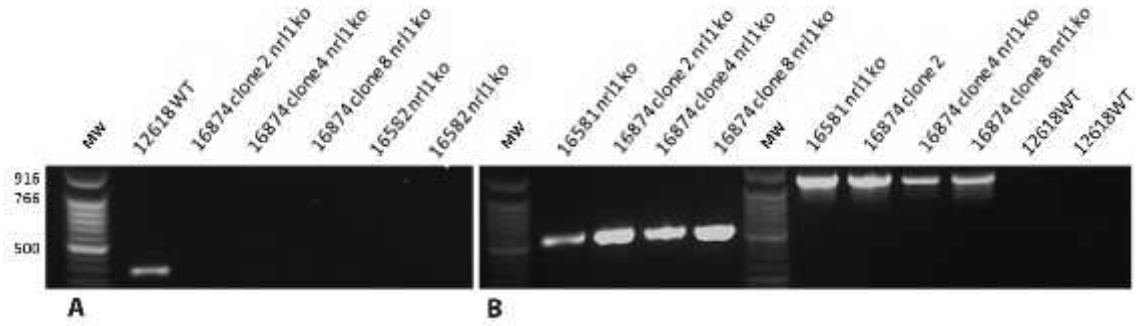

Figure 15 : Positive clones for nrl1 deletion. Colony PCR was performed from positive clones after transformation with pnko1 plasmid (A) pcr of the control strain 12618 and the positive transformant clones using WT primers. (B) PCR of positive transformant clones using the upch uni/upch and dwch/dwch uni primers respectively (834 and 534 bp), whose amplification will suggest presence of the insertion cassette. Strain 16581 was used as positive control for nrl1 knockout

III.2 Nrl1 is not required for centromere silencing by RNAi.

Since Nrl1 was originally identified in fission yeast as an orthologue of the RNAi protein NRDE-2 in *C. elegans*, then the first step would be to test whether it could also be required for RNAi silencing as its worm orthologue. In order to test this hypothesis, a centromeric silencing assay was performed using strains harbouring the marker ura4^{+} inserted either in the outermost repeat (omr1R) or innermost repeat (imr1R) on centromere of chromosome 1 **Error! Reference source not found.**(**Figure 16A**). For this, strains having a deletion or not in the *nrl1* gene (WT 12618 and *nrl1Δ* 16582) were used along with a strains having a deletion or not in the *swi6 gene* (WT 12618 and *swi6Δ* 17100), which would not be able to promote heterochromatin formation in the centromeric region if deleted. Three different media were used (**Figure 16B**), PMG as a positive control where all strain could grow, EMM-U (minimum media lacking Uracil), which served as a selection plate to indicate that only those strains that could transcribe the inserted ura4 marker (due to inhibition of heterochromatin formation) could grow. Finally, 5FOA plates were used to corroborate (as counter selection) what was observed in EMM-U plates and that was that only those strains with a silenced centromere could grow and those that would transcribe the inserted ura4 marker would accumulate the

toxic 5-fluoroacil due to the conversion made by the presence of uracil (transcriber product of the inserted marker).

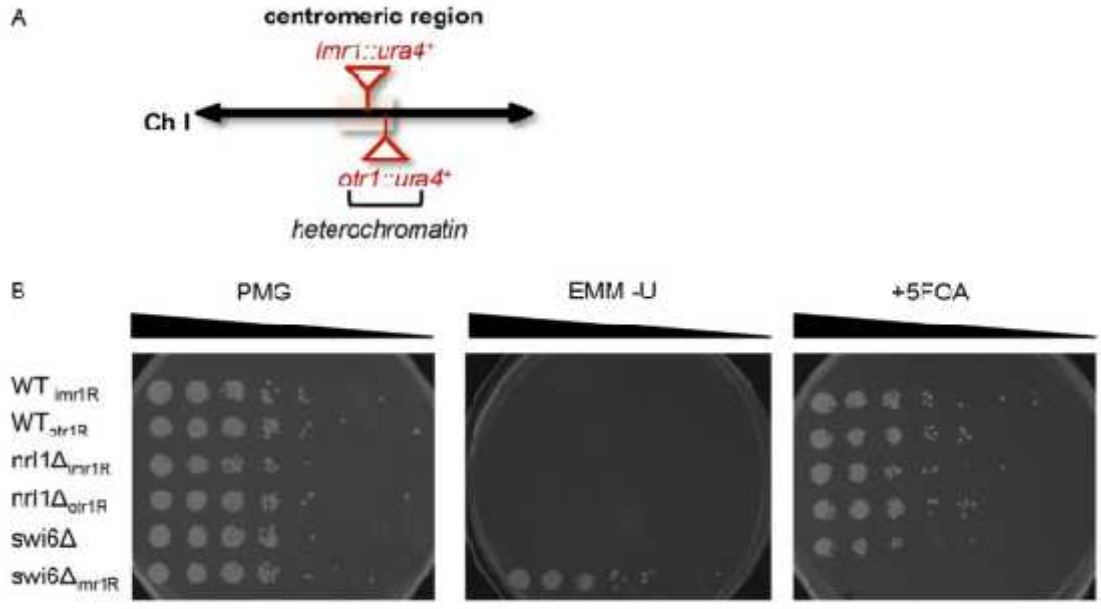

Figure 16 Figure. Nrl1 is not required for centromeric heterochromatin silencing (A) Schematic of the silencing assay. To monitor gene expression an ura4 marker was inserted in both WT and nrl1Δ strains in one of the following silenced loci: outermost repeat 1 right (otr1R) or innermost repeat 1 right (imr1R). (B) Strains constructed as shown in (A) were spotted onto selective medium lacking uracil (-U) or supplemented with 5-fluororotic acid (+5FOA) plates in five-fold dilution series.

According to the results observed in **Figure 16Error! Reference source not found.B,** it could be concluded that Nrl1 was not required to silence the inserted ura4 marker as the centromeric region remained heterochromatic with or without nrl1. The opposite was observed for the heterochromatic protein homologue Swi6, which was the responsible of heterochromatin formation in the centromeric region and therefore inhibiting the transcription of the inserted marker, making it possible to grow in 5FOA plates.

III.2.1 *Nrl1* deletion promotes activation of G2/M arrest by induction of chk1

Direct examination of nrl1 knockout by fluorescent microscopy revealed that *nrl1Δ* cells were elongated (average cell length = 16.4 µm) compared with wild-type cells (average cell length = 10.8µm) with a subpopulation of giant cells (3–5% of cells) reaching 30–50 µm (**Figure 17**). These findings were previously observed (45) and

additionally, cells exhibited nuclear fragmentation together with chromatin hypercondensation. This finding suggested that the cell cycle progression might be blocked preventing the cells to divide while being still able to undergo macromolecular synthesis and cell growth thus resulting in an elongated cell morphology. This phenotype has been previously observed in *S. pombe cdc* mutants that were able to grow but unable to undergo medial fission (4), perhaps providing the cell with time to repair its DNA.

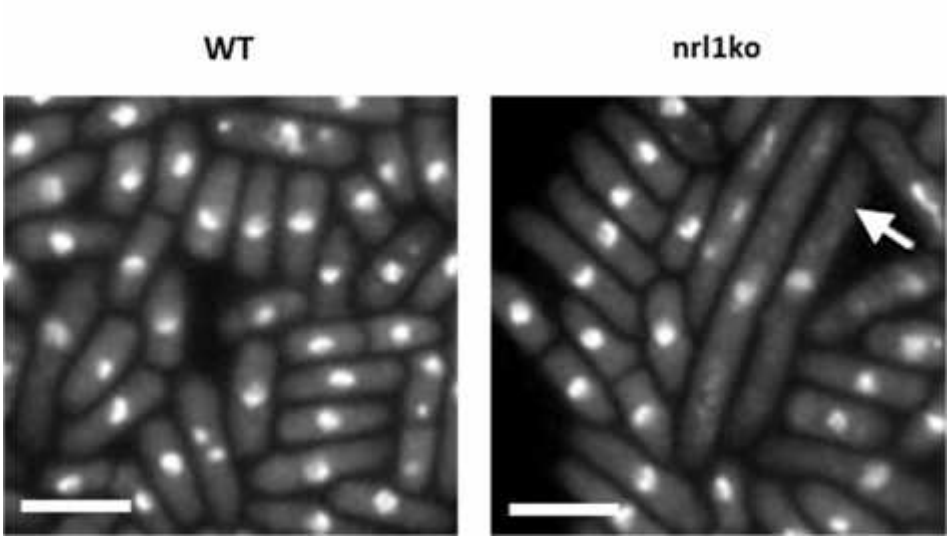

Figure 17 nrl1Δ strains showed 51% average increment in cell length. Deletion of nrl1 induced elongated morphology with a subpopulation of giant cells (white arrow) presumably by cell cycle arrest in S-phase before cells could undergo medial fission. Scale bar = 10 μm

Cell cycle checkpoints ensure that the integrity of genomic DNA is maintained throughout the cell cycle and in the event where DNA lesion occur, cell cycle is arrested until lesions are repaired and failure represents that cells have to mutate to overcome this control and continue to replicate and divide. This delay in the cell cycle represents an opportunity for the organism to pursue DNA repair (62). In fission yeast, Chk1 is an important protein kinase involved in the G2/M arrest, who is activated by the phosphorylation of its serine 345 in response to DNA damage, which is mediated by Rad3. This in turn, mediates phosphorylation of Cdc2, the main controller of G2/M transition in fission yeast, triggering cell cycle arrest. Another major cell cycle regulator is the intra-S phase checkpoint kinase Cds1 (Checking DNA Synthesis), which is homologous to Rad53 in budding yeast and Chk2 in mammals (63) and its function is to

phosphorylate further downstream targets regulating cell cycle progression and DNA repair mechanisms (64,65). Therefore deletion of either or the two (Chk1 and Cds1) result in checkpoints defects failing to properly arrest the cell cycle.

Subsequent studies (45) found that only in the presence of *nrl1Δ chk1Δ* double mutants the wild-type phenotype (average length of 9.8 μm) could be rescued with no detectable giant cells. Altogether, this findings indicate that loss of Nrl1 activates the DNA damage checkpoint resulting in Chk1-triggered G2/M arrest. Thus it is likely that Chk1 activation is triggered endogenously in a minority of cells reflecting the elongated G2-arrested subpopulation of *nrl1Δ*.

III.3 Nrl1 is not required for phosphorylation of RNA pol II during transcription

Since NRDE-2 in *C. elegans* has a role in transcription control through the inhibition of Pol II elongation, it was clear that the next step was to check whether Nrl1 might have the same function in *S. Pombe*. PolII elongation activity is regulated in the cell by the phosphorylation of Rpb1 CTD residues Ser5 and Ser2 respectively (39), while phosphorylation of Ser7 regulates snRNA transcription (44). Therefore it was decided to test the effects of nrl1 deletion on the phosphorylation levels of the serine 5,2, and 7 residues of the Rpb1 CTD. For this purpose, following TCA extraction of the different cell samples, a western blot was performed using specific antibodies against each of the serine residues of the RNA polII CTD (**Figure 18a**) and finally measure the band intensity and calculated the significance of the different phosphorylation values (**Figure 18b**)

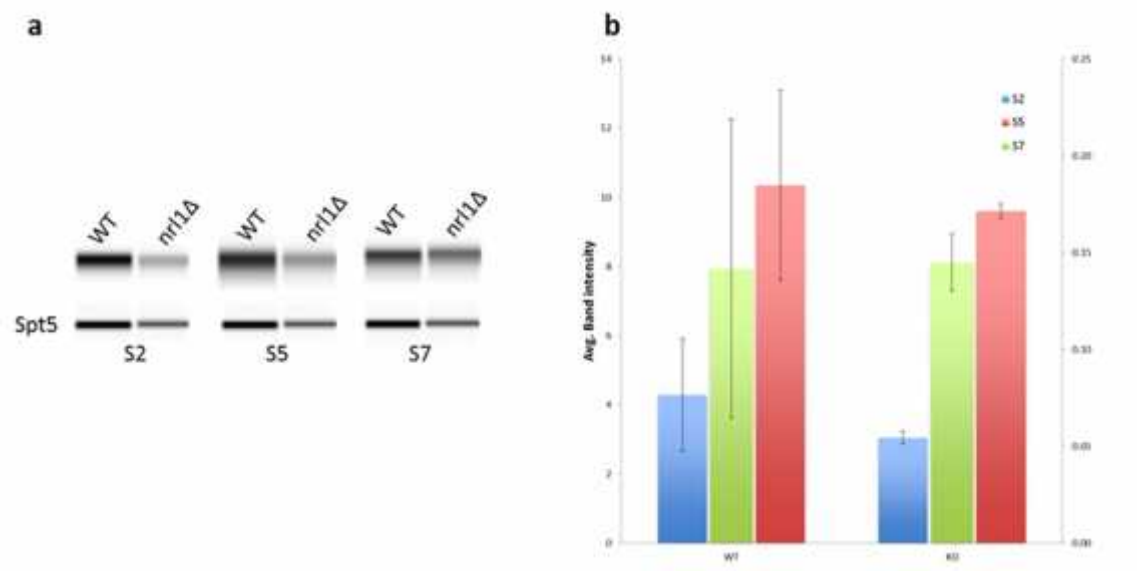

Figure 18 Nrl1 is not required for inhibition of RNA pol II elongation. a) Western blot of WT and nrl1Δ strains with and without radiation treatment. The bottom gel correspond to Anti-Spt5 used to normalize data b) Average band intensities of phosphorylation levels relative to Spt5 (loading control) were plotted against each strain regarding the antibodies against the serine residues of the RNA pol II CTD (blue for Ser2-P, red for Ser5-P and green for Ser7-P). Cells were grown until OD_{595} 0.4. S2, S5 and S7 corresponds to the specific antibody against the serine residue of RNA pol II.

No significant difference was found in the levels of the serine residues phosphorylation between the WT and nrl1Δ strains ($p>0.1$), suggesting that Nrl1 is not required for RNA polII transcription elongation. This results was in line with our previous finding that Nrl1 is not required for RNAi silencing like its worm orthologue.

III.4 Nrl1 associates with the spliceosome

III.4.1 TAP Tag purification of Nrl1

To analyze Nrl1 in its cellular context in *S. pombe*, Nrl1-associated factors were isolated by tandem affinity purification (TAP) of Nrl1-TAP tagged strains (17106), and the purified proteins were identified by mass spectrometry (MS) (66,67). TAP purification was performed both in presence and absence of RNase A to distinguish between core complex proteins and factors indirectly binding to Nrl1 through RNA-mediated interaction (**Figure 19**). Nrl1 copurified with an RNAse-resistant core complex consisting

of the pre-mRNA processing factors (**Figure 20**, **Table S1**) Mtl1 and Ctr1 and an RNAse-sensitive sub-complex including components of the U2·U5·U6 spliceosome and Prp19 complexes (68). These findings are consistent with a recent publication in which Nrl1 was shown to interact with spliceosome components (69). Importantly, Nrl1 did not co-purify with any RNAi factor, thus corroborating our previous finding that it was not required for RNAi silencing

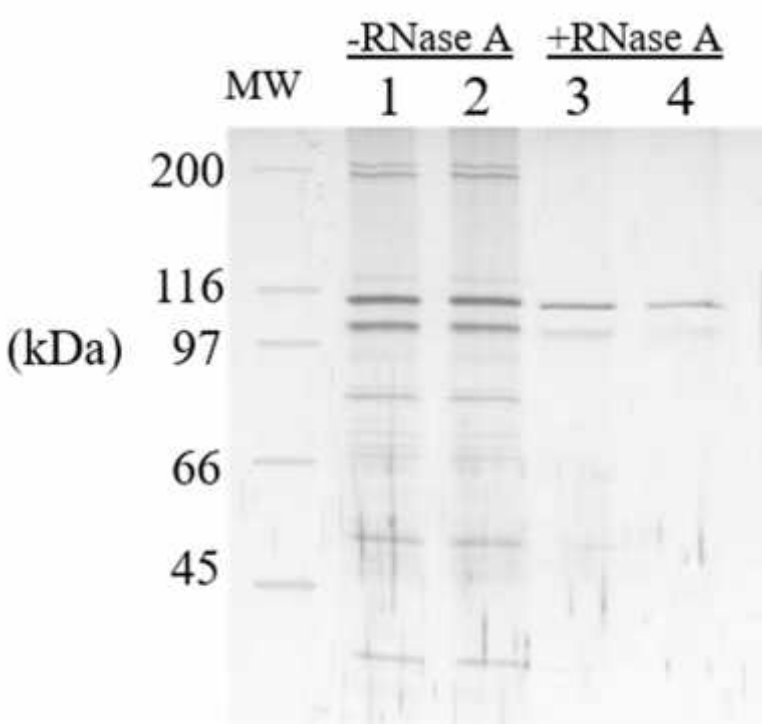

Figure 19 Tandem affinity purification of Nrl1. Tap tagged strains were purified following previously described methodology. l0 µl of protein fraction eluates from purifications carried out without RNase treatment (lane 1-2, - RNase A) or in presence of RNase (lane 3-4, +RNase A) were separated by SDS-GE and visualized by silver staining. Molecular weight markers (M marker) are indicated on the left.

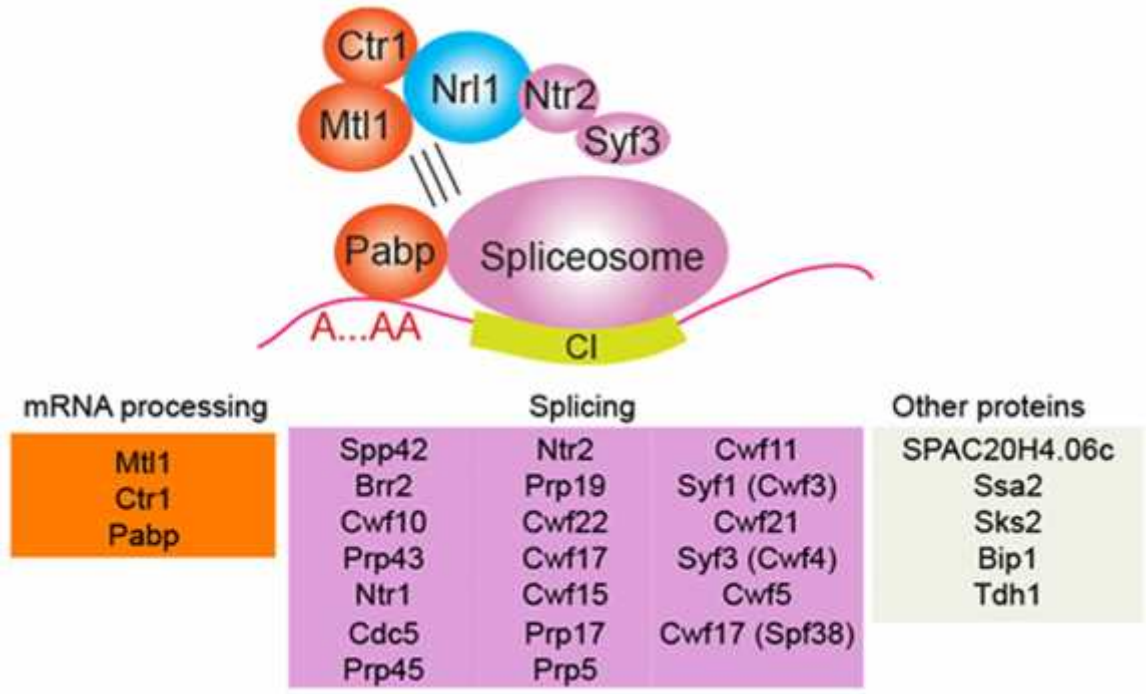

Figure 20. Nrl1 associates with spliceosome proteins. **Taken from Aronica et al (2015).** Nrl1-associated proteins were isolated from exponentially growing WT cells harbouring a TAP-tagged nrl1 allele (17106) in the presence or absence of RNase A by tandem affinity purification and identified by mass spectrometry (MS) analysis. A core complex consisting of Nrl1, Mtl1, Ctr1, Ntr2 and Syf3 associates through RNA-dependent interactions with the spliceosome. Blue: Nrl1; pink: splicing factors; orange: mRNA processing factors. Only the top 30 proteins based on spectral counting are shown.

III.4.2 Effects of Nrl1 depletion in transcription (RNA-seq)

III.4.2.1 Splicing analysis

Given that Nrl1 associates with spliceosome factors, it was examined whether Nrl1 might regulate pre-mRNA splicing. To this end, high-throughput paired-end sequencing of polyA+-selected mRNA (RNA-Seq) was performed from wild-type and *nrl1*Δ cells. To determine the differences on the splicing of introns, the 'percentage of spliced in' (PSI) was calculated by dividing the number of uniquely mapped exonic reads by the sum of uniquely mapped exonic reads and uniquely mapped splice junction reads spanning exon-exon borders. An intron was considered to be differentially spliced if there was a difference in its retention of more than 15% (ΔPSI>15 with a p-value ≤0.05) between wild-type and *nrl1Δ* cells. All introns obtained in our RNA-seq experiments were

evaluated, and 43 introns in protein-coding genes and non-coding RNAs met the criteria mentioned above (**Figure 21**, **Table S*2***). The affected genes were involved in a variety of processes including cellular transport and metabolism, transcription regulation and pre-mRNA processing. Together, these findings indicate that Nrl1 physically and functionally associates with the splicing machinery and its loss results in changes in the splicing patterns of a subset of introns.

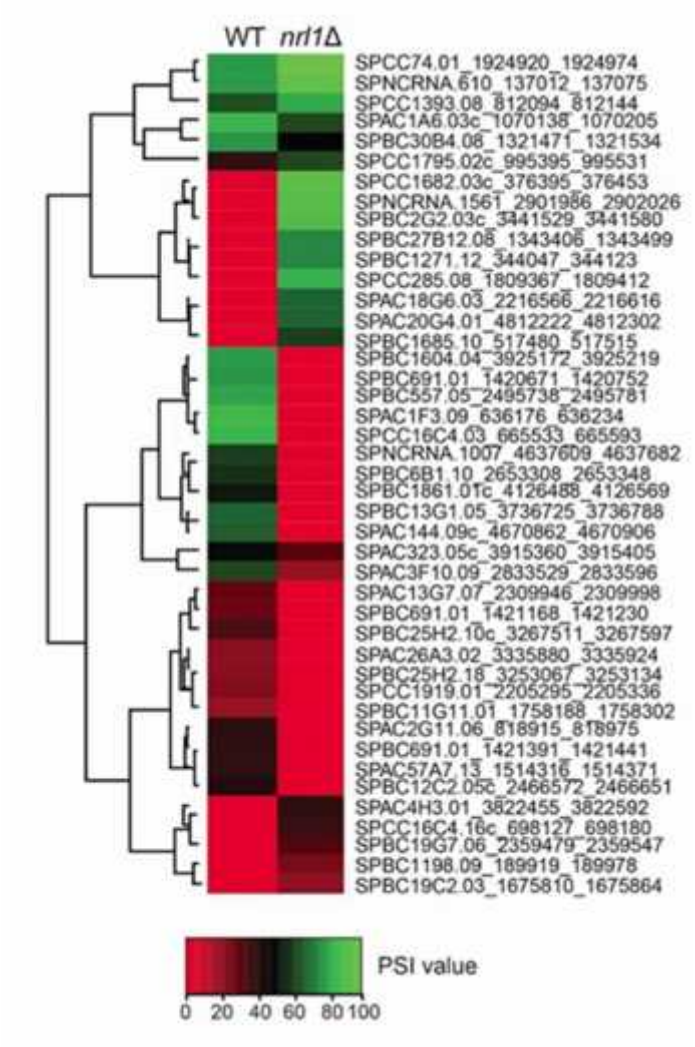

Figure 21. Nrl1 splicing defects. Taken from Aronica *et al* (2015). Heatmap of splicing changes by differences in the PSI values between WT and nrl1Δ. 43 genes displayed significant PSI differences between WT and nrl1Δ. Hierarchical clustering was performed using Euclidean distance. In each entry of the Heatmap the gene and the genomic coordinates of the respective intron are depicted. The heatmap was built using the gplots R package (heatmap. 2 function).

III.4.2.2 Nrl1 depletion affects expression transposable elements and meiotic genes

In addition to the splicing analysis, the expression patterns from both wild-type and *nrl1*Δ cells were observed by paired-end sequencing of polyA+-selected mRNA and observed that *nrl1* deletion resulted in the upregulation of transposable elements of the family Tf2 (Tf2-2, Tf2-7, Tf2-10, Tf2-11), the only family of full-length retro-transposons in fission yeast (**Figure 22**, **Table S3**) (70). Tf2 elements are primarily dependent on homologous recombination (71) and *S. pombe* applies a variety of defence mechanisms that restrict Tf2 activity to avoid chromosome instability and genome damage that results from increased copy number (72).

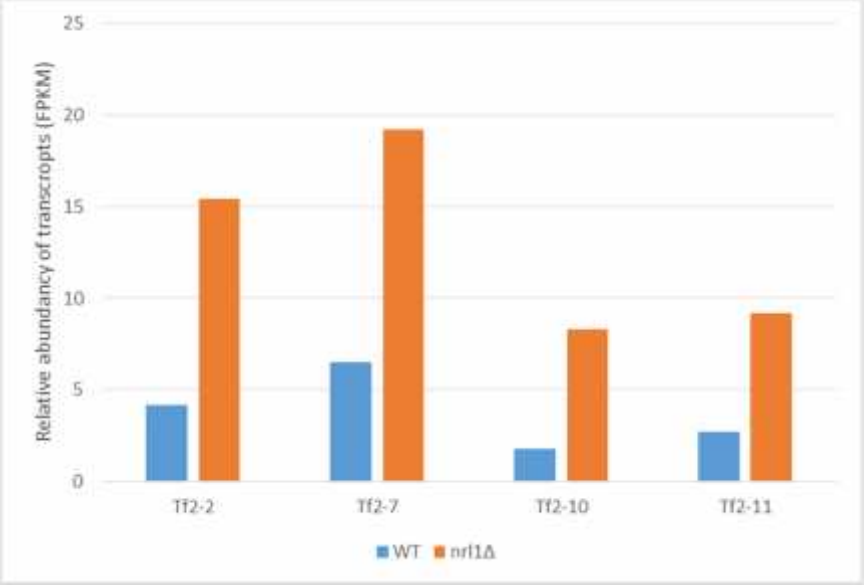

Figure 22. Transposable elements of the Tf2 family are upregulated in nrl1Δ. Differentially expressed Tf2 family genes between WT and nrl1Δ cells. Data were obtained by paired-end sequencing of polyA+-selected mRNA. Differences in gene expression were obtained using the Cufflinks-Cuffdiff software

In addition, deletion of *nrl1* affected the expression of several genes induced during meiosis, from the starvation response to the late meiotic phase (73). 70 out of 230 genes deregulated in *nrl1Δ* belonged to this category (**Figure 23**, **Table S3**). Starvation-induced genes required for the mating pheromone response and regulation of meiosis were all downregulated in *nrl1Δ*. These genes included: the guanine nucleotide-binding protein1 Gpa1 (74), the adaptor protein Ste4 (75), the MAP kinase

Spk1p (76), the regulator of G protein signaling Rgs1p (77), and the meiotic master regulator Mei2 (78). In contrast, the meiosis-specific kinetochore factor Moa1 was upregulated. This last is recruited by CENP-C to the centromere during MI (79) and is required for monopolar attachment during MI (80), a process in which sister kinetochores within one homologue attach to microtubules emanating from the same spindle pole.

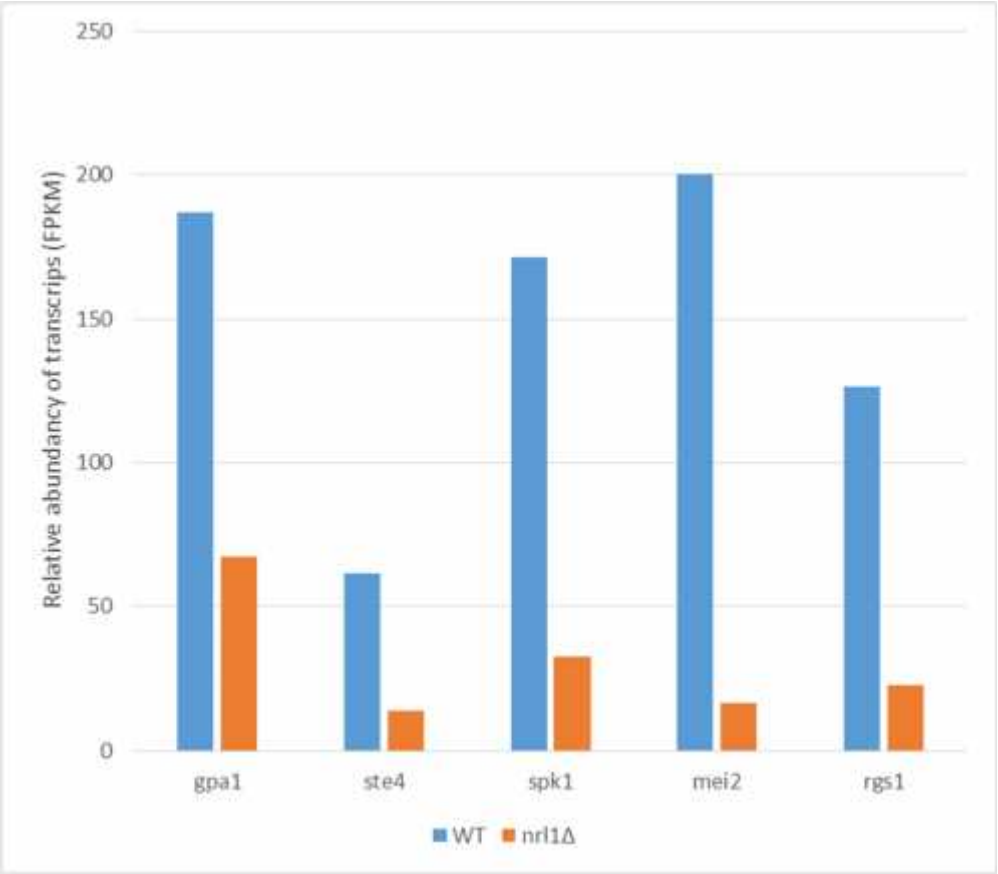

Figure 23. nrl1Δ depletion affected expression of meiotic genes. Differentially expressed meiotic genes between WT and nrl1Δ cells. Data were obtained by paired-end sequencing of polyA+-selected mRNA. Differences in gene expression were obtained using the Cufflinks-Cuffdiff software

III.5 Nrl1 deletion impairs proper chromosome segregation

These findings prompted us to further analyse the phenotype of *nrl1Δ* during meiosis. The aberrant expression of Moa1 and splicing of CENP-C in *nrl1Δ*, suggested that meiotic core centromere cohesion could be compromised in these strains. Centromere cohesion is required to hold sister chromatids together during anaphase I and prevent their separation until MII.

Therefore comparison of chromosome segregation and chromatid cohesion during MI in WT and *nrl1Δ* was performed by following the segregation of chromosome II marked by GFP close to centromere (cen2-GFP). To explore chromosome missegregation, mature asci formed from heterothallic strains were examined and then the GFP dots were scored according to the possible outcomes (**Figure 24**) by observation under fluorescence microscope

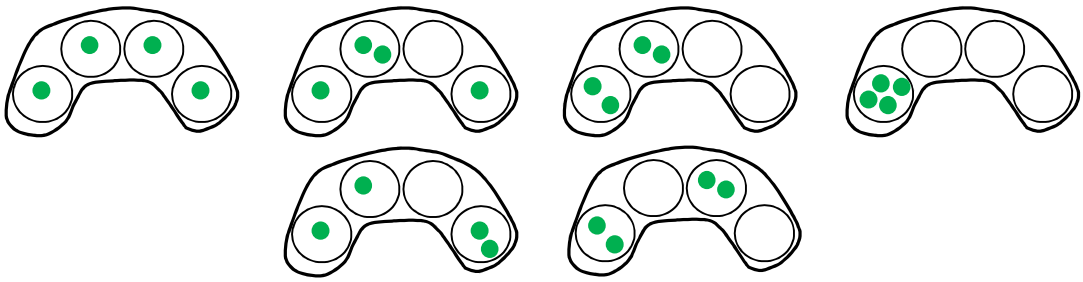

Figure 24. Possible outcomes of Chromosome II centromere segregation by visualization of expressed GPF marker inserted near the centromere.

To explore the behavior of sister chromatids, anaphase I (AI) was examined from cells derived from diploids generated by crossing an h+ strain harboring a cen2-GFP (16587) with an h- strain (16582) containing an unmarked chromosome II. These cells bear only one homolog marked by cen2-GFP, whose sister chromatids should segregate to the same spindle pole during AI. Strikingly, the percentage of aberrant sister segregation at AI markedly increased in *nrl1Δ* (15%) compared to WT levels (2%) ($p<0.05$). In addition, it was also found that up to 15% of h90 *nrl1Δ* cells had aberrant segregation (**Figure 25a, Figure 26**) compared to WT levels (2%), ($p<0.05$). As anticipated

from these results, *nrl1Δ* spores displayed a 30% lower viability and slower growth compared to WT strains. These data indicate that *nrl1Δ* suppresses the disjunction of sister centromeres during MI, probably by ensuring proper function of Moa1 and CENP-C.

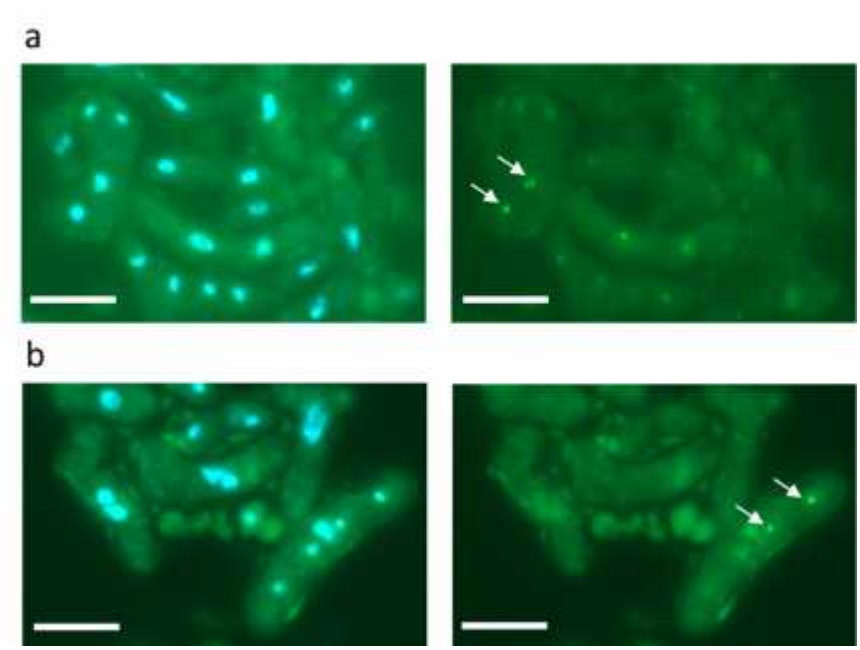

Figure 25 Nrl1Δ miss-segregation during Meiosis. Strains tagged with GPF in the centromere of the chromosome II (cen2-GFP) crossed and analysed by fluorescence microscopy (100x; Phase/DAPI and FITC) were scored for chromosome segregation. (a) miss-segregation of nrl1Δ strain 16873 by visualization expressed GFP marker (right picture). On the left, nuclei (stained with DAPI) of the same cell where chromosome miss-segregated can be observed. (b) Correct segregation of sister chromatids after heterothallic cross (16587 x 16582) where only one of the strains contained the GFP marker allowing analysis of Anaphase I.

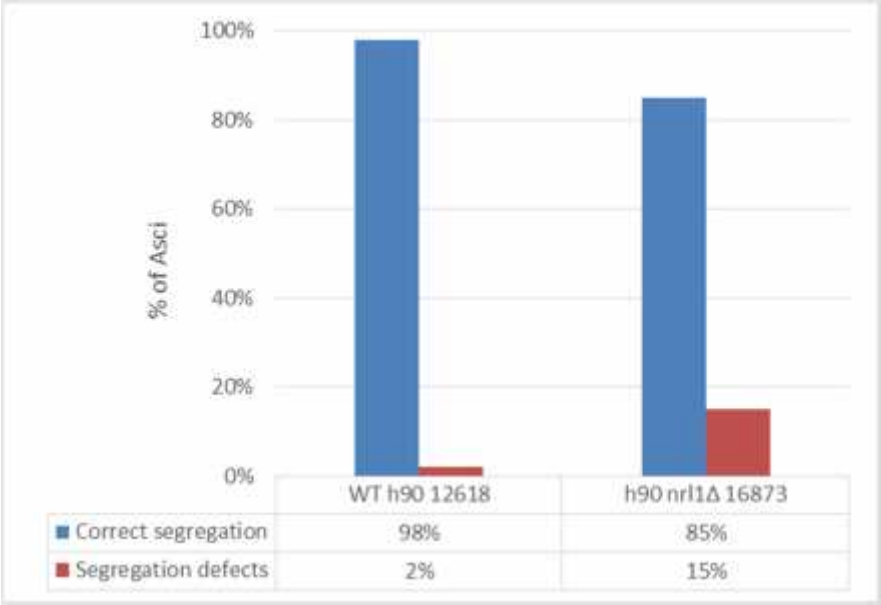

Figure 26 Deletion of Nrl1 mildly affects chromosome 2 segregation during meiosis II. Meiotic chromosome segregation of chromosome 2 was scored wild-type h90 cen2-GFP strain (12618) and h90 cen2-GFP strains with nrl1 deletion (16873)

The deregulation of meiotic genes in *nrl1Δ* and its phenotypic consequences on meiotic chromosome segregation and mating efficiency parallel the fertility defects observed in NRDE-2 mutants in *C. elegans* (81). Notably, also NRDE-2 has been implicated in a fertility pathway required for regulation of germ-line genes, germ-line chromosome segregation and transposon suppression.

III.6 Nrl1 analysis during meiosis

To further characterize the role of Nrl1 during meiosis, isolation Nrl1 protein complexes was carried out from meiotic cells using diploid strains harbouring Nrl1-TAP and *pat1-114* alleles (16927).

Pat1 kinase is a negative regulator of meiosis, and its major target is Mei2, an RNA-binding protein crucial for meiotic entry (78). Therefore, highly synchronous meiosis can be induced by inactivation of a temperature-sensitive allele of the Pat1 protein kinase (pat1-114), allowing cells to synchronously undergo premeiotic S phase followed by two rounds of chromosome segregation (meiosis I and meiosis II)

First, it was required to determine during which time-window Nrl1 was expressed at highest levels during meiosis with a high level of synchronized of cells in Meiosis. To this end, cells were first synchronized in G1 starvation in media lacking nitrogen source) and then inactivation of pat1 kinase (induction of meiosis) was performed by shifting from a permissive growth temperature of 25 °C to restrictive temperature of 34 °C in fresh media with nitrogen source. Then TCA extraction of nrl1 was performed upon meiosis in a timely and controlled manner by inactivating pat1 kinase during 1 hour intervals for a total of 5 hours and finally the progression of meiosis was monitored by flow cytometry for DNA content

It was found that at the onset of the fourth hour of incubation at non permissive temperature, the highest percentage of meiotic committed cells was obtained, which was in line with previous studies (82). Therefore, it was decided to perform Nrl1 TAP purification after 4 hours of meiotic induction by inactivation of pat1 Kinase. After MS analysis, no significant difference was found in the levels of expressions of Nrl1 between vegetative growing and meiotic cells. Interestingly, a different isoform of Nrl1 was observed (**Figure 27** lower band above 97kDa) suggesting that this might be a meiotic specific form of Nrl1 protein.

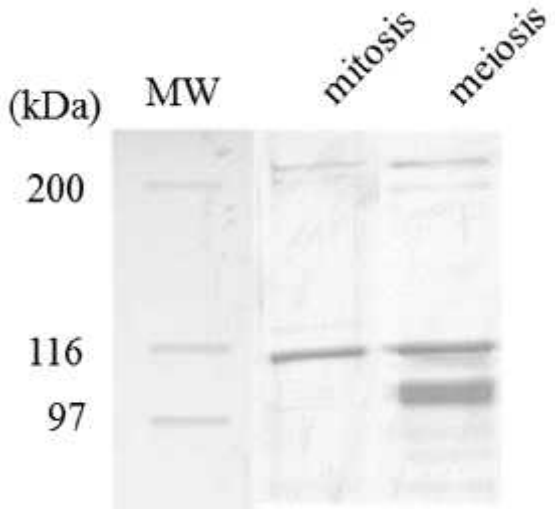

Figure 27 Tandem affinity purification of Nrl1 upon meiosis induction of pat1-114 strains. Tap tagged strains harbouring pat1-114 allele were purified following previously described methodology. l0 µl of protein fraction eluates from purifications were separated by SDS-GE and visualized by silver staining. Molecular weight markers (M marker) are indicated on the left.

Nrl1 complex does not significantly change in composition between vegetative and meiotic cells. Therefore, the role of Nrl1 during meiosis is not due to the recruitment of meiotic-specific factors, but it is likely mediated through its effects on the expression and splicing of meiotic specific genes as previously observed (**Figure 20**, **Table S4**).

IV CONCLUSIONS

Here a new functional insight on the role of the protein Nrl1 in pre-mRNA splicing and gene regulation is provided. Unlike its worm orthologue, the protein NRDE-2 of *C. elegans*, Nrl1 is not required for RNAi silencing and regulation of PolII elongation. Instead, it is shown that Nrl1 is associated with splicing and mRNA processing factors, is required for proper splicing of a subset of introns across the genome, and affects the expression of transposons and meiotic genes. Consistently with these findings, it was also observed that Nrl1 depletion results in significant defects in chromosome segregation during meiosis. Because the composition of Nrl1 associated protein complex does not significantly change between vegetative and meiotic cells, it is proposed that the effects of Nrl1 depletion during meiosis are due to its role in gene splicing and transcription. Since Nrl1 is conserved in higher eukaryotes including humans, the significance of this study reaches beyond the yeast system. The human orthologue of Nrl1, hNRDE-2, is downregulated and associated with Copy Number Aberrations (CNA) in tumor cells (83), suggesting that it may act as a tumor suppressor. Our findings provide a rationale for further investigating a possible role of hNRDE in regulation of gene expression in cancer.

V TABLE OF FIGURES

VI ACKNOWLEDGEMENTS

Renee Schroeder

for giving me the opportunity to work in this laboratory, for the help, patience and for her support during this time

Lucia Aronica

for being a great supervisor but mostly for being the greatest smallest human friend with a heart with the size of the sun, for instant help whenever I needed it and for giving me the freedom to work autonomously at the same time, for good advice and the creativity, for the helpful discussions and constructive comments on my thesis, for supporting and encouraging me, for the help and patience and never-ending optimism.

Dr. Juro Gregan

for his collaboration and for allowing me to work initially in his lab, for generously providing me the strains and chemicals, for his support, advice and helpful discussions.

Dr. Lubos Cipak

for his support and helpful discussions, for generously providing antibodies

To all Labkids

for squeezing themselves in order to provide a place to work, for their support, helpful discussions and motivation. Thank you Ivana for helping me not to blow the lab. Thank you Johanna for being the first aid. Thank you Katarzyna for your support, helpful discussions and tips. Thank you Meghan for your support and friendship and for acting as the mom of us all. Thank you Maximilian for being the best neighbour and your support. Thank you Nadia for your motivation and recognizing my hard work. Thank you Hakim for your support and helpful discussions. Thank you Adam for your support and for cheating on me with Chess and thank you Bob for your support

my family parents

for their unconditional love, support and effort to provide with their best in order for me to succeed professionally, for the mould that helped me become the man I am today.

my sister

for her support and interest despite my career was never her field, for her love

my M&Ms

for your support at all cost, for your patience and understanding during the moments I could not be a Husband and a Father. Thank you for the small details that always brought me joy, for your motivation, for being my motor. Thank you for being with me at all situations no matter the circumstances. Thank you for your time and love.

VII REFERENCES

1. Mitchison, J.M. (1957) The growth of single cells: I. Schizosaccharomyces pombe. *Experimental Cell Research*, **13**, 244-262.

2. Forsburg, S.L. (1999) The best yeast? *Trends in Genetics*, **15**, 340-344.

3. Forsburg, S.L. (2002) Only Connect: Linking Meiotic DNA Replication to Chromosome Dynamics. *Molecular Cell*, **9**, 703-711.

4. Forsburg, S.L. and Nurse, P. (1991) Cell Cycle Regulation in the Yeasts Saccharomyces cerevisiae and Schizosaccharomyces pombe. *Annual Review of Cell Biology*, **7**, 227-256.

5. Forsburg, S. (2004), Vol. 2016, pp. DNA replication and research at the Forsburg Lab, as well as practical information, protocols and reference pages for working with fission yeast, internet guides to pombe, sequence analysis.

6. Wood, V., Gwilliam, R., Rajandream, M.A., Lyne, M., Lyne, R., Stewart, A., Sgouros, J., Peat, N., Hayles, J., Baker, S. *et al.* (2002) The genome sequence of Schizosaccharomyces pombe. *Nature*, **415**, 871-880.

7. Allshire, R.C. (1995) Elements of chromosome structure and function in fission yeast. *Seminars in Cell Biology*, **6**, 55-64.

8. Smirnova, J.B. and McFarlane, R.J. (2002) The unique centromeric chromatin structure of Schizosaccharomyces pombe is maintained during meiosis. *J Biol Chem*, **277**, 19817-19822.

9. Kloc, A. and Martienssen, R. (2008) RNAi, heterochromatin and the cell cycle. *Trends Genet*, **24**, 511-517.

10. Colmenares, S.U., Buker, S.M., Buhler, M., Dlakić, M. and Moazed, D. (2007) Coupling of Double-Stranded RNA Synthesis and siRNA Generation in Fission Yeast RNAi. *Molecular Cell*, **27**, 449-461.

11. Irvine, D.V., Zaratiegui, M., Tolia, N.H., Goto, D.B., Chitwood, D.H., Vaughn, M.W., Joshua-Tor, L. and Martienssen, R.A. (2006) Argonaute Slicing Is Required for Heterochromatic Silencing and Spreading. *Science*, **313**, 1134-1137.

12. Buker, S.M., Iida, T., Buhler, M., Villen, J., Gygi, S.P., Nakayama, J.-I. and Moazed, D. (2007) Two different Argonaute complexes are required for siRNA generation and heterochromatin assembly in fission yeast. *Nat Struct Mol Biol*, **14**, 200-207.

13. Verdel, A. and Moazed, D. (2005) RNAi-directed assembly of heterochromatin in fission yeast. *FEBS Lett*, **579**, 5872-5878.

14. Yamada-Inagawa, T., Klar, A.J.S. and Dalgaard, J.Z. (2007) Schizosaccharomyces pombe Switches Mating Type by the Synthesis-Dependent Strand-Annealing Mechanism. *Genetics*, **177**, 255-265.

15. Holmes, A.M., Kaykov, A. and Arcangioli, B. (2005) Molecular and Cellular Dissection of Mating-Type Switching Steps in Schizosaccharomyces pombe. *Molecular and Cellular Biology*, **25**, 303-311.

16. Mercer, T.R., Dinger, M.E. and Mattick, J.S. (2009) Long non-coding RNAs: insights into functions. *Nat Rev Genet*, **10**, 155-159.

17. Allo, M., Buggiano, V., Fededa, J.P., Petrillo, E., Schor, I., de la Mata, M., Agirre, E., Plass, M., Eyras, E., Elela, S.A. *et al.* (2009) Control of alternative splicing through siRNA-mediated transcriptional gene silencing. *Nat Struct Mol Biol*, **16**, 717-724.

18. Ting, A.H., Schuebel, K.E., Herman, J.G. and Baylin, S.B. (2005) Short dsRNA Induces Transcriptional Gene Silencing in Human Cancer Cells in the Absence of DNA Methylation. *Nature genetics*, **37**, 906-910.

19. Morris, K.V., Chan, S.W.L., Jacobsen, S.E. and Looney, D.J. (2004) Small Interfering RNA-Induced Transcriptional Gene Silencing in Human Cells. *Science*, **305**, 1289-1292.

20. Chen, E.S., Zhang, K., Nicolas, E., Cam, H.P., Zofall, M. and Grewal, S.I.S. (2008) Cell cycle control of centromeric repeat transcription and heterochromatin assembly. *Nature*, **451**, 734-737.

21. Djupedal, I., Portoso, M., Spåhr, H., Bonilla, C., Gustafsson, C.M., Allshire, R.C. and Ekwall, K. (2005) RNA Pol II subunit Rpb7 promotes centromeric transcription and RNAi-directed chromatin silencing. *Genes & Development*, **19**, 2301-2306.

22. Kato, H., Goto, D.B., Martienssen, R.A., Urano, T., Furukawa, K. and Murakami, Y. (2005) RNA Polymerase II Is Required for RNAi-Dependent Heterochromatin Assembly. *Science*, **309**, 467-469.

23. Bayne, E.H., Portoso, M., Kagansky, A., Kos-Braun, I.C., Urano, T., Ekwall, K., Alves, F., Rappsilber, J. and Allshire, R.C. (2008) Splicing factors facilitate RNAi-directed silencing in fission yeast. *Science*, **322**, 602-606.

24. Chinen, M., Morita, M., Fukumura, K. and Tani, T. (2010) Involvement of the spliceosomal U4 small nuclear RNA in heterochromatic gene silencing at fission yeast centromeres. *J Biol Chem*, **285**, 5630-5638.

25. Li, C.F., Pontes, O., El-Shami, M., Henderson, I.R., Bernatavichute, Y.V., Chan, S.W.L., Lagrange, T., Pikaard, C.S. and Jacobsen, S.E. An ARGONAUTE4-Containing Nuclear Processing Center Colocalized with Cajal Bodies in Arabidopsis thaliana. *Cell*, **126**, 93-106.

26. Pontes, O., Li, C.F., Nunes, P.C., Haag, J., Ream, T., Vitins, A., Jacobsen, S.E. and Pikaard, C.S. The Arabidopsis Chromatin-Modifying Nuclear siRNA Pathway Involves a Nucleolar RNA Processing Center. *Cell*, **126**, 79-92.

27. Birchler, J.A., Gao, Z. and Han, F. (2008) A tale of two centromeres—diversity of structure but conservation of function in plants and animals. *Functional & Integrative Genomics*, **9**, 7-13.

28. Kavi, H.H. and Birchler, J.A. (2009) Interaction of RNA polymerase II and the small RNA machinery affects heterochromatic silencing in Drosophila. *Epigenetics & Chromatin*, **2**, 15-15.

29. Brower-Toland, B., Findley, S.D., Jiang, L., Liu, L., Yin, H., Dus, M., Zhou, P., Elgin, S.C.R. and Lin, H. (2007) Drosophila PIWI associates with chromatin and interacts directly with HP1a. *Genes & Development*, **21**, 2300-2311.

30. Guang, S., Bochner, A.F., Burkhart, K.B., Burton, N., Pavelec, D.M. and Kennedy, S. (2010) Small regulatory RNAs inhibit RNA polymerase II during the elongation phase of transcription. *Nature*, **465**, 1097-1101.

31. Allo, M., Buggiano, V., Fededa, J.P., Petrillo, E., Schor, I., de la Mata, M., Agirre, E., Plass, M., Eyras, E., Elela, S.A. *et al.* (2009) Control of alternative splicing through siRNA-mediated transcriptional gene silencing. *Nat Struct Mol Biol*, **16**, 717-724.

32. Kim, D.H., Sætrom, P., Snøve, O. and Rossi, J.J. (2008) MicroRNA-directed transcriptional gene silencing in mammalian cells. *Proceedings of the National Academy of Sciences*, **105**, 16230-16235.

33. Zhang, K., Mosch, K., Fischle, W. and Grewal, S.I.S. (2008) Roles of the Clr4 methyltransferase complex in nucleation, spreading and maintenance of heterochromatin. *Nat Struct Mol Biol*, **15**, 381-388.

34. Tay, Y., Zhang, J., Thomson, A.M., Lim, B. and Rigoutsos, I. (2008) MicroRNAs to Nanog, Oct4 and Sox2 coding regions modulate embryonic stem cell differentiation. *Nature*, **455**, 1124-1128.

35. Mitsuzawa, H. and Ishihama, A. (2003) RNA polymerase II transcription apparatus in Schizosaccharomyces pombe. *Current Genetics*, **44**, 287-294.

36. Heidemann, M., Hintermair, C., Voß, K. and Eick, D. (2013) Dynamic phosphorylation patterns of RNA polymerase II CTD during transcription.

Biochimica et Biophysica Acta (BBA) - Gene Regulatory Mechanisms, **1829**, 55-62.

37. Stump, A.D. and Ostrozhynska, K. (2013) Selective constraint and the evolution of the RNA Polymerase II C-Terminal Domain. *Transcription*, **4**, 77-86.

38. Eick, D. and Geyer, M. (2013) The RNA Polymerase II Carboxy-Terminal Domain (CTD) Code. *Chemical Reviews*, **113**, 8456-8490.

39. Bowman, E.A. and Kelly, W.G. (2014) RNA Polymerase II transcription elongation and Pol II CTD Ser2 phosphorylation: A tail of two kinases. *Nucleus*, **5**, 224-236.

40. Spåhr, H., Calero, G., Bushnell, D.A. and Kornberg, R.D. (2009) Schizosacharomyces pombe RNA polymerase II at 3.6-Å resolution. *Proceedings of the National Academy of Sciences*, **106**, 9185-9190.

41. Egloff, S. and Murphy, S. (2008) Cracking the RNA polymerase II CTD code. *Trends in Genetics*, **24**, 280-288.

42. Komarnitsky, P., Cho, E.-J. and Buratowski, S. (2000) Different phosphorylated forms of RNA polymerase II and associated mRNA processing factors during transcription. *Genes & Development*, **14**, 2452-2460.

43. Kim, H., Erickson, B., Luo, W., Seward, D., Graber, J.H., Pollock, D., Megee, P.C. and Bentley, D.L. (2010) Gene-specific RNA pol II phosphorylation and the "CTD code". *Nature structural & molecular biology*, **17**, 1279-1286.

44. Egloff, S., O'Reilly, D., Chapman, R.D., Taylor, A., Tanzhaus, K., Pitts, L., Eick, D. and Murphy, S. (2007) Serine 7 of the RNA polymerase II CTD is specifically required for snRNA gene expression. *Science (New York, N.Y.)*, **318**, 1777-1779.

45. Aronica, L., Kasparek, T., Ruchman, D., Marquez, Y., Cipak, L., Cipakova, I., Anrather, D., Mikolaskova, B., Radtke, M., Sarkar, S. *et al.* (2015) The spliceosome-associated protein Nrl1 suppresses homologous recombination-dependent R-loop formation in fission yeast. *Nucleic Acids Research*.

46. Hanahan, D. and Weinberg, Robert A. Hallmarks of Cancer: The Next Generation. *Cell*, **144**, 646-674.

47. Malkova, A. and Haber, J.E. (2012) Mutations Arising During Repair of Chromosome Breaks. *Annual Review of Genetics*, **46**, 455-473.

48. Skourti-Stathaki, K. and Proudfoot, N.J. (2014) A double-edged sword: R loops as threats to genome integrity and powerful regulators of gene expression. *Genes & Development*, **28**, 1384-1396.

49. Thomas, M., White, R.L. and Davis, R.W. (1976) Hybridization of RNA to double-stranded DNA: formation of R-loops. *Proceedings of the National Academy of Sciences of the United States of America*, **73**, 2294-2298.

50. Lenzken, S.C., Loffreda, A. and Barabino, S.M.L. (2013) RNA Splicing: A New Player in the DNA Damage Response. *International Journal of Cell Biology*, **2013**, 153634.

51. Sato, Y., Yoshizato, T., Shiraishi, Y., Maekawa, S., Okuno, Y., Kamura, T., Shimamura, T., Sato-Otsubo, A., Nagae, G., Suzuki, H. *et al.* (2013) Integrated molecular analysis of clear-cell renal cell carcinoma. *Nat Genet*, **45**, 860-867.

52. Gregan, J., Rabitsch, P.K., Rumpf, C., Novatchkova, M., Schleiffer, A. and Nasmyth, K. (2006) High-throughput knockout screen in fission yeast. *Nature protocols*, **1**, 2457-2464.

53. Goldstein, A.L. and McCusker, J.H. (1999) Three new dominant drug resistance cassettes for gene disruption in Saccharomyces cerevisiae. *Yeast*, **15**, 1541-1553.

54. Cipak, L., Hyppa, R.W., Smith, G.R. and Gregan, J. (2012) ATP analog-sensitive Pat1 protein kinase for synchronous fission yeast meiosis at physiological temperature. *Cell Cycle*, **11**, 1626-1633.

55. Bradford, M.M. (1976) A rapid and sensitive method for the quantitation of microgram quantities of protein utilizing the principle of protein-dye binding. *Analytical Biochemistry*, **72**, 248-254.

56. Puig, O., Caspary, F., Rigaut, G., Rutz, B., Bouveret, E., Bragado-Nilsson, E., Wilm, M. and Seraphin, B. (2001) The tandem affinity purification (TAP) method: a general procedure of protein complex purification. *Methods*, **24**, 218-229.

57. Lyne, R., Burns, G., Mata, J., Penkett, C.J., Rustici, G., Chen, D., Langford, C., Vetrie, D. and Bähler, J. (2003) Whole-genome microarrays of fission yeast: characteristics, accuracy, reproducibility, and processing of array data. *BMC Genomics*, **4**, 1-15.

58. Zhong, S., Joung, J.G., Zheng, Y., Chen, Y.R., Liu, B., Shao, Y., Xiang, J.Z., Fei, Z. and Giovannoni, J.J. (2011).

59. Trapnell, C., Pachter, L. and Salzberg, S.L. (2009) TopHat: discovering splice junctions with RNA-Seq. *Bioinformatics*, **25**, 1105-1111.

60. Trapnell, C., Roberts, A., Goff, L., Pertea, G., Kim, D., Kelley, D.R., Pimentel, H., Salzberg, S.L., Rinn, J.L. and Pachter, L. (2012) Differential gene and transcript expression analysis of RNA-seq experiments with TopHat and Cufflinks. *Nat. Protocols*, **7**, 562-578.

61. Yamamoto, A. and Hiraoka, Y. (2003) Monopolar spindle attachment of sister chromatids is ensured by two distinct mechanisms at the first meiotic division in fission yeast. *The EMBO Journal*, **22**, 2284-2296.

62. Hartwell, L. and Weinert, T. (1989) Checkpoints: controls that ensure the order of cell cycle events. *Science*, **246**, 629-634.

63. Murakami, H. and Okayama, H. (1995) A kinase from fission yeast responsible for blocking mitosis in S phase. *Nature*, **374**, 817-819.

64. Matsuoka, S., Huang, M. and Elledge, S.J. (1998) Linkage of ATM to Cell Cycle Regulation by the Chk2 Protein Kinase. *Science*, **282**, 1893-1897.

65. Enoch, T., Carr, A.M. and Nurse, P. (1992) Fission yeast genes involved in coupling mitosis to completion of DNA replication. *Genes & Development*, **6**, 2035-2046.

66. Rigaut, G., Shevchenko, A., Rutz, B., Wilm, M., Mann, M. and Seraphin, B. (1999) A generic protein purification method for protein complex characterization and proteome exploration. *Nat Biotechnol*, **17**, 1030-1032.

67. Cipak, L., Spirek, M., Novatchkova, M., Chen, Z., Rumpf, C., Lugmayr, W., Mechtler, K., Ammerer, G., Csaszar, E. and Gregan, J. (2009) An improved strategy for tandem affinity purification-tagging of Schizosaccharomyces pombe genes. *Proteomics*, **9**, 4825-4828.

68. Chen, W., Shulha, H.P., Ashar-Patel, A., Yan, J., Green, K.M., Query, C.C., Rhind, N., Weng, Z. and Moore, M.J. (2014) Endogenous U2.U5.U6 snRNA complexes in S. pombe are intron lariat spliceosomes. *RNA*, **20**, 308-320.

69. Lee, N.N., Chalamcharla, V.R., Reyes-Turcu, F., Mehta, S., Zofall, M., Balachandran, V., Dhakshnamoorthy, J., Taneja, N., Yamanaka, S., Zhou, M. *et al.* (2013) Mtr4-like protein coordinates nuclear RNA processing for heterochromatin assembly and for telomere maintenance. *Cell*, **155**, 1061-1074.

70. Bowen, N.J., Jordan, I.K., Epstein, J.A., Wood, V. and Levin, H.L. (2003) Retrotransposons and their recognition of pol II promoters: a comprehensive survey of the transposable elements from the complete genome sequence of Schizosaccharomyces pombe. *Genome research*, **13**, 1984-1997.

71. Hoff, E.F., Levin, H.L. and Boeke, J.D. (1998) Schizosaccharomyces pombe Retrotransposon Tf2 Mobilizes Primarily through Homologous cDNA Recombination. *Molecular and Cellular Biology*, **18**, 6839-6852.

72. Esnault, C. and Levin, H.L. (2015) The Long Terminal Repeat Retrotransposons Tf1 and Tf2 of Schizosaccharomyces pombe. *Microbiology Spectrum*, **3**.

73. Mata, J., Lyne, R., Burns, G. and Bähler, J. (2002) The transcriptional program of meiosis and sporulation in fission yeast. *Nat Genet*, **32**.

74. Fourmann, J.-B., Schmitzová, J., Christian, H., Urlaub, H., Ficner, R., Boon, K.-L., Fabrizio, P. and Lührmann, R. (2013) Dissection of the factor requirements for spliceosome disassembly and the elucidation of its dissociation products using a purified splicing system. *Genes & Development*, **27**, 413-428.

75. Barr, M.M., Tu, H., Van Aelst, L. and Wigler, M. (1996) Identification of Ste4 as a potential regulator of Byr2 in the sexual response pathway of Schizosaccharomyces pombe. *Molecular and cellular biology*, **16**, 5597-5603.

76. Jones, K.B., Salah, Z., Del Mare, S., Galasso, M., Gaudio, E., Nuovo, G.J., Lovat, F., LeBlanc, K., Palatini, J., Randall, R.L. *et al.* (2012) miRNA Signatures Associate with Pathogenesis and Progression of Osteosarcoma. *Cancer Research*, **72**, 1865-1877.

77. Pereira, P.S. and Jones, N.C. (2001) The RGS domain-containing fission yeast protein, Rgs1p, regulates pheromone signalling and is required for mating. *Genes to Cells*, **6**, 789-802.

78. Watanabe, Y. and Yamamoto, M. (1994) S. pombe mei2+ encodes an RNA-binding protein essential for premeiotic DNA synthesis and meiosis I, which cooperates with a novel RNA species meiRNA. *Cell*, **78**.

79. Tanaka, K., Chang, H.L., Kagami, A. and Watanabe, Y. (2009) CENP-C functions as a scaffold for effectors with essential kinetochore functions in mitosis and meiosis. *Developmental cell*, **17**, 334-343.

80. Yokobayashi, S. and Watanabe, Y. (2005) The kinetochore protein Moa1 enables cohesion-mediated monopolar attachment at meiosis I. *Cell*, **123**, 803-817.

81. Sakaguchi, A., Sarkies, P., Simon, M., Doebley, A.L., Goldstein, L.D., Hedges, A., Ikegami, K., Alvares, S.M., Yang, L., LaRocque, J.R. *et al.* (2014) Caenorhabditis elegans RSD-2 and RSD-6 promote germ cell immortality by maintaining small interfering RNA populations. *Proceedings of the National Academy of Sciences of the United States of America*.

82. Bähler, J., Schuchert, P., Grimm, C. and Kohli, J. (1991) Synchronized meiosis and recombination in fission yeast: observations with pat1-114 diploid cells. *Current Genetics*, **19**, 445-451.

83. Chiu, C.G., Nakamura, Y., Chong, K.K., Huang, S.K., Kawas, N.P., Triche, T., Elashoff, D., Kiyohara, E., Irie, R.F., Morton, D.L. *et al.* (2014) Genome-Wide Characterization of Circulating Tumor Cells Identifies Novel Prognostic Genomic Alterations in Systemic Melanoma Metastasis. *Clinical Chemistry*, **60**, 873-885.

VIII APENDIX

VIII.1 Supplementary Methods and Data

Table S1 List of Nrl1 associated proteins in exponentially growing cells both in presence and absence of RNaseA.

Protein ID	Fasta headers	Number of proteins	Razor + unique peptides minus RNase	Razor + unique peptides plus RNASe	Mol. weight [kDa]	Sequence lengths
Most abundant proteins						
SPBC20F10.05	>SPBC20F10.05 |nrl1||NRDE-2 family protein |Schizosacch	1	42	44	113.25	972
SPAC140.04	>SPAC140.04 |||conserved eukaryotic protein|Schizosacch	1	29	30	35.323	295
SPAC17H9.02;SPA	>SPAC17H9.02 |||TRAMP complex ATP-dependent RNA he	2	48	48	118.46	1030;1117
Porteins with reduced levels upon RNase treatment						
SPAC4F8.12c	>SPAC4F8.12c |spp42|cwf6|U5 snRNP complex subunit Spp	1	44	14	274.55	2363
SPAC9.03c	>SPAC9.03c |brr2|spp41|U5 snRNP complex subunit Brr2 |	1	32	9	248.81	2176
SPAC1486.03c	>SPAC1486.03c |||RNA-binding splicing factor |Schizosacch	1	21	8	91.668	797
SPBC16H5.10c;SP	>SPBC16H5.10c |prp43||ATP-dependent RNA helicase Prp4	3	25	9	83.803	735;1168;117
SPBC215.12;SPCP	>SPBC215.12 |cwf10|spef2, snu114|GTPase Cwf10 |Schizos	3	24	6	111.31	984;842;842
SPAC29A4.08c	>SPAC29A4.08c |prp19|cwf8|ubiquitin-protein ligase E4|S	1	13	5	54.191	488
SPAC20H4.06c	>SPAC20H4.06c |||RNA-binding protein|Schizosaccharomy	1	20	1	60.763	534
SPAC644.12	>SPAC644.12 |cdc5||cell division control protein, splicing f	1	24	3	86.843	757
SPBC13E7.01	>SPBC13E7.01 |cwf22|SPBC15D4.16|splicing factor Cwf22|	1	14	0	102.7	886
SPBC6B1.10	>SPBC6B1.10 |prp17||splicing factor Prp17|Schizosaccharo	1	10	1	63.132	558
SPCC188.11	>SPCC188.11 |prp45|cwf13, snw1, SPCC584.08|splicing fact	1	16	5	62.696	557
SPBC1289.11	>SPBC1289.11 |spf38|cwf17|splicing factor Spf38|Schizosa	1	8	3	37.427	340
SPCC576.11;SPAC	>SPCC576.11 |rpl15||60S ribosomal protein L15 |Schizosac	2	6	2	23.806	201;201
SPCC550.02c	>SPCC550.02c |cwf5|ecm2|RNA-binding protein Cwf5|Sch	1	9	0	39.576	354
SPAC3A12.10;SPA	>SPAC3A12.10 |rpl2001|rpl20-1, rpl20, yl17b, rpl18a-2|60S	2	7	2	20.599	176;176
SPAC17A2.08c	>SPAC17A2.08c |Ntr2| |||sequence orphan|Schizosacchar	1	7	2	41.874	361
SPBC19C2.14	>SPBC19C2.14 |smd3||Sm snRNP core protein Smd3|Schiz	1	3	2	11.033	97
SPCC364.03	>SPCC364.03 |rpl1702|rpl17-2, rpl17|60S ribosomal protein	1	7	1	20.827	187
SPAC4A8.09c	>SPAC4A8.09c |cwf21||complexed with Cdc5 protein Cwf2	1	7	0	34.553	293
SPBC211.02c	>SPBC211.02c |cwf3|syf1|complexed with Cdc5 protein Cw	1	3	0	92.636	790
SPAC2C4.03c	>SPAC2C4.03c |smd2|cwf9|Sm snRNP core protein Smd2|S	1	3	0	13.095	115

Table S2. Genes showing significant difference in Percentage of Spliced Introns (PSI) in nrl1Δ vs WT cells

Gene_id	Chr	Start intron	End intron	Status intron	Samples	PSI sample 1	PSI sample 2	ΔPSI	P-value ΔPSI
SPCC1682.03c	III	376395	376453	NEW	WT_nrl1	0	90.48	90.479	2.2e-16
SPNCRNA.1561	II	2901986	2902026	NEW	WT_nrl1	0	88.89	88.889	2.2e-16
SPBC2G2.03c	II	3441529	3441580	ANNOTATED	WT_nrl1	0	86.67	86.669	2.2e-16
SPAC1F3.09	I	636176	636234	ANNOTATED	WT_nrl1	83.33	0	83.329	9.923e-08
SPCC16C4.03	III	665533	665593	NEW	WT_nrl1	80.95	0	80.949	0.006911
SPCC285.08	III	1809367	1809412	ANNOTATED	WT_nrl1	0	79.17	79.169	2.2e-16
SPBC557.05	II	2495738	2495781	ANNOTATED	WT_nrl1	76.47	0	76.469	0.01303
SPBC1604.04	II	3925172	3925219	ANNOTATED	WT_nrl1	75.34	0	75.339	4.197e-14
SPBC691.01	II	1420671	1420752	ANNOTATED	WT_nrl1	75	0	74.999	0.003906
SPBC1271.12	II	344047	344123	ANNOTATED	WT_nrl1	0	72.22	72.219	2.2e-16
SPBC27B12.08	II	1343406	1343499	ANNOTATED	WT_nrl1	0	72.22	72.219	2.2e-16
SPAC18G6.03	I	2216566	2216616	NEW	WT_nrl1	0	65.52	65.519	2.2e-16
SPAC20G4.01	I	4812222	4812302	ANNOTATED	WT_nrl1	0	65.38	65.379	2.2e-16
SPBC13G1.05	II	3736725	3736788	ANNOTATED	WT_nrl1	65	0	64.999	0.0006434
SPAC144.09c	I	4670862	4670906	ANNOTATED	WT_nrl1	64.71	0	64.709	0.0006822
SPBC1685.10	II	517480	517515	NEW	WT_nrl1	0	58.82	58.819	2.2e-16
SPNCRNA.1007	I	4637609	4637682	NEW	WT_nrl1	58.82	0	58.819	0.02875
SPBC6B1.10	II	2653308	2653348	ANNOTATED	WT_nrl1	57.14	0	57.139	0.002656
SPBC1861.01c	II	4126488	4126569	ANNOTATED	WT_nrl1	51.52	0	51.519	0.0001688
SPAC3F10.09	I	2833529	2833596	ANNOTATED	WT_nrl1	60.61	18.42	42.19	9.679e-14
SPBC12C2.05c	II	2466572	2466651	ANNOTATED	WT_nrl1	40.48	0	40.479	3.186e-09
SPAC2G11.06	I	818915	818975	ANNOTATED	WT_nrl1	38.89	0	38.889	0.0004666
SPBC691.01	II	1421391	1421441	ANNOTATED	WT_nrl1	38.46	0	38.459	0.002708
SPAC4H3.01	I	3822455	3822592	NEW	WT_nrl1	0	38.24	38.239	2.2e-16
SPAC57A7.13	I	1514316	1514371	ANNOTATED	WT_nrl1	37.84	0	37.839	0.0009438
SPCC16C4.16c	III	698127	698180	ANNOTATED	WT_nrl1	0	36.67	36.669	2.2e-16
SPBC25H2.10c	II	3267511	3267597	ANNOTATED	WT_nrl1	32.26	0	32.259	0.0003083
SPBC19G7.06	II	2359479	2359547	ANNOTATED	WT_nrl1	0	31.58	31.579	2.2e-16
SPAC13G7.07	I	2309946	2309998	ANNOTATED	WT_nrl1	27.78	0	27.779	0.04185
SPBC30B4.08	II	1321471	1321534	ANNOTATED	WT_nrl1	75	48.39	26.61	0.001436
SPBC691.01	II	1421168	1421230	ANNOTATED	WT_nrl1	25.64	0	25.639	7.204e-06
SPBC1198.09	II	189919	189978	ANNOTATED	WT_nrl1	0	22.95	22.949	2.2e-16
SPCC1919.01	III	2205295	2205336	ANNOTATED	WT_nrl1	22.43	0	22.429	2.672e-06
SPAC1A6.03c	I	1070138	1070205	ANNOTATED	WT_nrl1	82.35	60	22.35	0.007203
SPCC1795.02c	III	995395	995531	NEW	WT_nrl1	38.1	60	21.9	0.00899
SPAC26A3.02	I	3335880	3335924	ANNOTATED	WT_nrl1	21.05	0	21.049	0.0004971
SPBC25H2.18	II	3253067	3253134	ANNOTATED	WT_nrl1	20.99	0	20.989	0.000826
SPBC19C2.03	II	1675810	1675864	ANNOTATED	WT_nrl1	0	19.28	19.279	2.2e-16
SPCC74.01	III	1924920	1924974	ANNOTATED	WT_nrl1	76.32	95.56	19.24	0.001199
SPAC323.05c	I	3915360	3915405	ANNOTATED	WT_nrl1	49.09	30.56	18.53	0.02976
SPBC11G11.01	II	1758188	1758302	ANNOTATED	WT_nrl1	17.86	0	17.859	0.005976
SPNCRNA.610	I	137012	137075	NEW	WT_nrl1	75.9	92.59	16.69	0.000135
SPCC1393.08	III	812094	812144	NEW	WT_nrl1	62.28	78.49	16.21	0.001202

Table S3. Differentially expressed genes between WT and *nrl1Δ*. Differences in gene expression were obtained using the Cufflinks-Cuffdiff software

Gene ID	gene	locus	WT	nrl1Δ	log2 (fold change)	p-value
SPCC548.07c	ght1	III:232287-239381	862.356	13.7933	-5.96624	5e-05
SPAPB24D3.10c	agl1	I:2967915-2976287	660.75	15.8577	-5.38085	5e-05
SPBC359.06	mug14	II:122656-129742	884.753	21.7037	-5.34926	5e-05
SPAC1F8.01	ght3	I:82745-84786	172.268	6.39979	-4.75049	5e-05
SPCC191.11	inv1	III:1723392-1727277	681.568	40.6753	-4.06663	5e-05
SPAC27D7.03c	mei2	I:4510982-4515015	200.367	16.6522	-3.58886	5e-05
SPBC1683.08	ght4	II:151489-159570	125.763	14.8074	-3.08632	5e-05
SPBC20F10.04c	nse4	II:3287674-3301277	53.0837	440.254	3.052	5e-05
SPAC22A12.11	dak1	I:1172208-1180072	967.428	133.102	-2.86162	5e-05
SPAC22F3.12c	rgs1	I:678570-681890	126.614	22.958	-2.46337	5e-05
SPAC31G5.09c	spk1	I:2998748-3001687	171.305	32.4001	-2.40249	5e-05
SPAC4G9.13c	vps26	I:2276858-2279439	555.897	119.243	-2.22091	5e-05
SPBC1E8.04	Tf2-10	II:1965389-1969387	1.79595	8.31412	2.21082	5e-05
SPCC1235.14	ght5	III:212159-214376	2601.9	564.415	-2.20474	5e-05
SPAC1F7.07c	fip1	I:4232997-4234760	11.3905	50.9288	2.16065	5e-05
SPAC1565.04c	ste4	I:1294071-1296634	61.7196	13.8834	-2.15237	0.0001
SPBC1861.02	abp2	II:4126317-4133635	8.52846	36.1437	2.08339	5e-05
SPAC167.08	Tf2-2	I:1564100-1568523	4.14784	15.4063	1.89309	5e-05
SPAC30D11.01c	gto2	I:1119879-1123773	176.291	48.534	-1.86089	5e-05
SPCC1020.10	oca2	III:757329-763615	13.7373	48.7715	1.82794	5e-05
SPBC1198.02	dea2	II:174821-177244	51.3506	182.266	1.82759	5e-05
SPBC4F6.09	str1	II:2704644-2707648	13.3657	46.7991	1.80794	5e-05
SPBC1289.17	Tf2-11	II:4414656-4418658	2.73356	9.18404	1.74835	5e-05

SPCC1753.02c	git3	III:1542332-1554681	184.135	56.9888	-1.69202	5e-05
SPBC4B4.08	ght2	II:3427179-3429424	55.0944	175.217	1.66917	5e-05
SPBC1604.01	egt1	II:3928129-3933343	265.737	84.339	-1.65573	5e-05
SPAP7G5.04c	lys1	I:3736519-3743579	102.487	321.874	1.65105	5e-05
SPAC4F8.07c	hxk2	I:2662987-2667395	1452.54	465.813	-1.64076	5e-05
SPAC13F5.03c	gld1	I:2174640-2185990	215.52	70.9879	-1.60218	0.0013
SPAC22G7.06c	ura1	I:739166-746117	83.4675	251.035	1.5886	5e-05
SPAC13D1.01c	Tf2-7	I:5191059-5195702	6.49149	19.2122	1.5654	5e-05
SPBPB2B2.12c	gal10	II:4482233-4487569	61.7525	20.9729	-1.55797	5e-05
SPCC548.06c	ght8	III:226335-230546	113.608	333.654	1.55429	5e-05
SPAC513.03	mfm2	I:2912761-2913270	79.0235	231.642	1.55154	5e-05
SPBC1773.05c	tms1	II:288555-292250	132.245	45.1753	-1.54961	0.00085
SPBC428.11	met17	II:465474-467823	165.943	478.845	1.52887	5e-05
SPBC24C6.06	gpa1	II:2327363-2331890	187.143	67.3564	-1.47425	5e-05
SPBC16E9.01c	php4	II:1915374-1916974	7.70624	20.3506	1.40097	5e-05
SPBC17F3.01c	rga5	II:2486558-2488209	12.4914	32.8677	1.39574	5e-05
SPBC32H8.02c	nep2	II:1451330-1454730	15.9341	41.5003	1.381	5e-05
SPAC869.11	cat1	I:5489133-5491791	43.0557	111.84	1.37716	5e-05
SPCC1682.09c	gcg1	III:388527-390514	33.9067	85.1049	1.32767	5e-05
SPBC947.04	pfl3	II:669580-673842	5.61646	13.8893	1.30624	5e-05
SPAC3C7.14c	obr1	I:2089236-2095865	651.189	1609.3	1.30528	5e-05
SPAC1F7.08	fio1	I:4235079-4237874	12.7388	31.3086	1.29733	5e-05
SPAPJ760.03c	adg1	I:5265434-5269973	122.461	300.61	1.29557	5e-05
SPAC664.09	ggt1	I:1718919-1721701	18.9929	46.4998	1.29176	5e-05
SPBC17D1.06	dbp3	II:3338603-3346442	64.7114	157.709	1.28517	5e-05
SPBP26C9.03c	fet4	II:327423-331064	9.74522	23.5847	1.27509	5e-05

SPAC1399.03	fur4	I:1841907-1843995	41.2371	99.4176	1.26956	5e-05
SPBC359.02	alr2	II:107513-109353	84.9702	35.5584	-1.25677	5e-05
SPAC29B12.08	clr5	I:5419732-5431523	13.5085	32.1047	1.24892	0.0009
SPAC5H10.06c	adh4	I:156429-158279	53.6112	127.217	1.24668	5e-05
SPBC1347.02	fkbp39	II:4061231-4065960	58.5709	137.829	1.23463	5e-05
SPCC18B5.01c	bfr1	III:709301-715435	44.1812	102.674	1.21657	5e-05
SPCC1393.10	ctr4	III:818301-819361	192.76	442.965	1.20039	5e-05
SPAC3C7.08c	elf1	I:2079069-2082533	52.3041	118.622	1.18138	5e-05
SPAC1F8.05	isp3	I:95158-96966	113.761	50.1764	-1.18093	5e-05
SPRRNA.01	21S_rRNA	MT:0-2822	72.0195	31.7839	-1.18009	5e-05
SPBC2D10.06	rep1	II:2976694-2979469	15.421	6.89219	-1.16186	0.00065
SPAC57A10.12c	ura3	I:1385356-1387063	124.9	278.017	1.1544	5e-05
SPBP35G2.16c	ecl2	II:961006-963780	491.738	223.946	-1.13474	5e-05
SPAC2F3.17c	lsm6	I:3923585-3924176	172.962	79.2552	-1.12588	0.00015
SPAC8F11.10c	pvg1	I:2869643-2871785	549.345	252.489	-1.12149	0.00025
SPBC106.17c	cys2	II:409157-413409	86.3077	187.307	1.11784	0.00055
SPRRNA.02	15S_rRNA	MT:3130-4552	107.811	50.0696	-1.1065	0.00035
SPBC16E9.16c	lsd90	II:1947984-1950255	158.658	73.8333	-1.10357	0.0007
SPBC27B12.11c	pho7	II:1345111-1347969	10.7563	22.8482	1.0869	5e-05
SPBC36.04	cys11	II:847929-851518	87.1958	184.965	1.08492	5e-05
SPBC1D7.02c	scr1	II:1752099-1755619	15.0925	31.8617	1.07799	0.0001
SPCC1672.02c	sap1	III:559678-565519	167.519	351.028	1.06726	0.0004
SPCC1020.09	gnr1	III:763666-767541	75.7336	157.669	1.0579	0.00025
SPAP7G5.02c	gua2	I:3733591-3735652	376.252	783.093	1.05749	0.0001
SPAC20G8.03	itr2	I:1393607-1398272	793.291	381.229	-1.05719	0.00135
SPAC25B8.01	dap1	I:4155464-4156320	147.538	70.9935	-1.05532	5e-05

SPAC23C4.11	atp18	I:1046858-1048934	31.5986	15.4084	-1.03614	0.00065
SPBC119.10	asn1	II:734995-737295	451.363	923.704	1.03314	0.00035
SPCC1840.12	opt3	III:2280652-2284409	17.1042	34.744	1.02242	0.0002
SPBC29B5.02c	isp4	II:1550292-1553467	105.65	52.4822	-1.00939	0.00125
SPCC757.09c	rnc1	III:62685-66972	118.01	236.098	1.00048	0.0002
SPBC27B12.03c	erg32	II:1323522-1325832	39.4816	78.6063	0.993467	5e-05
SPBC23G7.08c	rga7	II:2109253-2113453	5.28275	10.5018	0.99128	5e-05
SPAC821.09	eng1	I:998685-1002361	113.374	225.017	0.988943	0.00095
SPCC777.09c	arg1	III:1613046-1616219	367.253	727.325	0.985826	0.0006
SPAC1093.01	ppr5	I:4604710-4611737	34.3341	67.8406	0.982509	5e-05
SPBC23G7.04c	nif1	II:2101253-2103827	14.4684	28.4413	0.975078	5e-05
SPBC56F2.09c	arg5	II:4094157-4096292	238.555	468.827	0.974733	0.00075
SPBC337.16	cho1	II:1058346-1059126	605.968	314.726	-0.945147	0.00015
SPCC965.07c	gst2	III:2294616-2296383	273.085	524.069	0.940407	0.00075
SPBC4C3.05c	nuc1	II:3127775-3133199	49.7357	93.1382	0.905092	0.0005
SPCC1840.01c	mog1	III:2247360-2248273	127.75	68.3389	-0.902542	5e-05
SPAC4G8.13c	prz1	I:786777-792274	32.2287	60.0345	0.897443	0.0009
SPAC1F8.06	fta5	I:99045-101431	6.79277	12.6497	0.897036	5e-05
SPBC2G2.08	ade9	II:3448864-3453406	30.5201	56.657	0.892497	5e-05
SPNCRNA.67	prl67	III:1431047-1435036	31.5335	58.5132	0.891876	0.00045
SPAC806.07	ndk1	I:247719-248560	323.361	174.869	-0.886867	0.0002
SPBC1778.01c	zuo1	II:3094848-3096383	258.213	475.44	0.880701	0.0005
SPBC1539.09c	trp1	II:4377220-4379500	79.5372	143.646	0.852812	0.0004
SPCC1259.05c	cox9	III:1042383-1043131	184.847	102.83	-0.846077	0.00025
SPCC1223.08c	dfr1	III:1855306-1857115	40.718	73.131	0.844817	0.00055
SPAC630.11	vps55	I:366633-367890	233.295	131.003	-0.832563	0.00025

SPAC1142.05	ctr5	I:3635142-3636572	80.3194	142.487	0.827006	0.00055
SPAC25B8.02	sds3	I:4156471-4157726	24.7313	43.8683	0.82684	0.0008
SPAC11E3.09	pyp3	I:5298655-5300189	84.5374	47.6606	-0.826794	0.00055
SPAC29B12.10c	pgt1	I:5431574-5434908	31.9738	56.3914	0.818586	0.0004
SPAC16C9.03	nmd3	I:794865-796821	30.7505	53.9789	0.811785	0.0002
SPBC31F10.15c	atp15	II:3783855-3784529	385.827	220.282	-0.8086	0.00065
SPBC1683.10c	pcl1	II:163533-165317	188.416	108.59	-0.795025	0.0003
SPAC15A10.04c	zpr1	I:3683596-3685385	84.8494	146.756	0.790446	0.0005
SPBC1289.05c	vma10	II:4391436-4392721	500.801	289.94	-0.788482	0.0004
SPAC17A2.12	rrp1	I:3576768-3583005	2.84493	4.8797	0.778402	0.0009
SPBC19F8.07	mcs6	II:3243308-3244568	84.8617	49.5033	-0.777587	0.00125
SPCC1450.07c	dao1	III:1736499-1738318	20.6247	34.9089	0.759224	0.00055
SPAC20G8.09c	nat10	I:1415451-1418825	23.6131	39.6034	0.746036	0.00095
SPCC4E9.02	cig1	III:1227173-1229303	22.4719	37.6591	0.744879	0.00045
SPAC12B10.16c	mug157	I:4601277-4603478	109.406	66.3148	-0.722292	0.0013
SPAC23C4.13	bet1	I:1051664-1052724	199.274	121.99	-0.707996	0.00105
SPBC19C7.09c	uve1	II:2837571-2840744	48.7359	29.8778	-0.70591	0.00155
SPAC15E1.07c	moa1	I:3728515-3729034	0	1.13665	inf	0.00165
SPMTR.01	matPc	MTR:3353-3753	55.0286	0	-inf	5e-05

Table S4. List of Nrl1 associated proteins in cells upon 4 hours of meiosis induction by inactivation of pat1 kinase.

Identified Proteins (134)	Acc Num	MW	Nrl1 Meiosis
|||TRAMP complex ATP-dependent RNA helicase |Schizosaccharomyces pombe|chr 1|||Manual	SPAC17H9.02	118 kDa	28
|||NRDE-2 family, implicated in RNA interference|Schizosaccharomyces pombe|chr 2|||Manual	SPBC20F10.05	113 kDa	25
|||conserved eukaryotic protein|Schizosaccharomyces pombe|chr 1|||Manual	SPAC140.04	35 kDa	21
|spp42|cwf6|U5 snRNP complex subunit Spp42|Schizosaccharomyces pombe|chr 1|||Manual	SPAC4F8.12c	275 kDa	22
|cwf10|spef2, snu114|GTPase Cwf10 |Schizosaccharomyces pombe|chr 2|||Manual	SPBC215.12	111 kDa	14
|brr2|spp41|U5 snRNP complex subunit Brr2 |Schizosaccharomyces pombe|chr 1|||Manual	SPAC9.03c	249 kDa	16
|cdc5||cell division control protein, splicing factor Cdc5|Schizosaccharomyces pombe|chr 1|||Manual	SPAC644.12	87 kDa	8
|||RNA-binding protein|Schizosaccharomyces pombe|chr 1|||Manual	SPAC20H4.06c	61 kDa	5
|prp45|cwf13, snw1, SPCC584.08|splicing factor Prp45|Schizosaccharomyces pombe|chr 3|||Manual	SPCC188.11	63 kDa	5
|ssa2||heat shock protein Ssa2 |Schizosaccharomyces pombe|chr 3|||Manual	SPCC1739.13	70 kDa	10
|prp43||ATP-dependent RNA helicase Prp43 |Schizosaccharomyces pombe|chr 2|||Manual	SPBC16H5.10c	84 kDa	12
|||RNA-binding splicing factor |Schizosaccharomyces pombe|chr 1|||Manual	SPAC1486.03c	92 kDa	8
|prp19|cwf8|ubiquitin-protein ligase E4|Schizosaccharomyces pombe|chr 1|||Manual	SPAC29A4.08c	54 kDa	5
|pabp||mRNA export shuttling protein|Schizosaccharomyces pombe|chr 1|||Manual	SPAC57A7.04c	72 kDa	0
|prp17||splicing factor Prp17|Schizosaccharomyces pombe|chr 2|||Manual	SPBC6B1.10	63 kDa	3

|rpl8||60S ribosomal protein L7a/L8 |Schizosaccharomyces pombe|chr 2|||Manual	SPBC29A3.04	29 kDa	8
|cwf22|SPBC15D4.16|splicing factor Cwf22|Schizosaccharomyces pombe|chr 2|||Manual	SPBC13E7.01	103 kDa	1
|cwf15||complexed with Cdc5 protein Cwf15|Schizosaccharomyces pombe|chr 2|||Manual	SPBC337.06c	30 kDa	2
|||sequence orphan|Schizosaccharomyces pombe|chr 1|||Manual	SPAC17A2.08c	31 kDa	4
|rpl301|rpl3-1, rpl3|60S ribosomal protein L3|Schizosaccharomyces pombe|chr 1|||Manual	SPAC17A5.03 (+1)	44 kDa	8
|rpl13||60S ribosomal protein L13 |Schizosaccharomyces pombe|chr 1|||Manual	SPAC664.05	24 kDa	4
|prp5|cwf1|WD repeat protein Prp5|Schizosaccharomyces pombe|chr 2|||Manual	SPBP22H7.07	52 kDa	3
|rps13||40S ribosomal protein S13 |Schizosaccharomyces pombe|chr 1|||Manual	SPAC6F6.07c	17 kDa	3
|rpl35||60S ribosomal protein L35|Schizosaccharomyces pombe|chr 3|||Manual	SPCC613.05c	14 kDa	3
|spf38|cwf17|splicing factor Spf38|Schizosaccharomyces pombe|chr 2|||Manual	SPBC1289.11	37 kDa	3
|cwf3|syf1|complexed with Cdc5 protein Cwf3|Schizosaccharomyces pombe|chr 2|||Manual	SPBC211.02c	93 kDa	1
|cwf21||complexed with Cdc5 protein Cwf21|Schizosaccharomyces pombe|chr 1|||Manual	SPAC4A8.09c	35 kDa	2
|rpl3601|rpl36-1|60S ribosomal protein L36|Schizosaccharomyces pombe|chr 3|||Manual	SPCC970.05	11 kDa	3
|rpl402|rpl4-2, rpl4|60S ribosomal protein L2 |Schizosaccharomyces pombe|chr 2|||Manual	SPBP8B7.03c	40 kDa	7
|rps102|rps1-2, rps3a-2|40S ribosomal protein S3a |Schizosaccharomyces pombe|chr 1|||Manual	SPAC22H12.04c	29 kDa	6
|cwf5|ecm2|RNA-binding protein Cwf5|Schizosaccharomyces pombe|chr 3|||Manual	SPCC550.02c	40 kDa	3

|cwf11||complexed with Cdc5 protein Cwf11|Schizosaccharomyces pombe|chr 2|||Manual	SPBC646.02	148 kDa	0
|rpl801|rpl8-1, rpl18, rpk5a, rpl2-1, SPAC21E11.02c|60S ribosomal protein L8 |Schizosaccharomyces pombe|chr 1|||Manual	SPAC1F7.13c	27 kDa	5
|cwf4|syf3|complexed with Cdc5 protein Cwf4|Schizosaccharomyces pombe|chr 2|||Manual	SPBC31F10.11c	81 kDa	0
|tdh1|gpd1|glyceraldehyde-3-phosphate dehydrogenase Tdh1|Schizosaccharomyces pombe|chr 2|||Manual	SPBC32F12.11	36 kDa	4
|rpl26||60S ribosomal protein L26 |Schizosaccharomyces pombe|chr 2|||Manual	SPBC29B5.03c	14 kDa	3
|rpl2001|rpl20-1, rpl20, yl17b, rpl18a-2|60S ribosomal protein L20a |Schizosaccharomyces pombe|chr 1|||Manual	SPAC3A12.10	21 kDa	3
|cwf2|prp3|RNA-binding protein Cwf2|Schizosaccharomyces pombe|chr 1|||Manual	SPAC3A12.11c	44 kDa	0
|rpl44|rpl28|60S ribosomal protein L28/L44 |Schizosaccharomyces pombe|chr 1|||Manual	SPAC1687.06c	15 kDa	4
|cwf12||complexed with Cdc5 protein Cwf12|Schizosaccharomyces pombe|chr 2|||Manual	SPBC32F12.05c	26 kDa	2
|rpl1901|rpl19-1|60S ribosomal protein L19|Schizosaccharomyces pombe|chr 2|||Manual	SPBC56F2.02 (+1)	23 kDa	5
|rpl6||60S ribosomal protein L6 |Schizosaccharomyces pombe|chr 3|||Manual	SPCC622.18	21 kDa	4
|rpl1802|rpl18-2|60S ribosomal protein L18 |Schizosaccharomyces pombe|chr 1|||Manual	SPAPB17E12.13	21 kDa	3
|rps1701|rps17-1|40S ribosomal protein S17 |Schizosaccharomyces pombe|chr 2|||Manual	SPBC839.05c	16 kDa	3
|rpl3702|rpl37-2, rpl37|60S ribosomal protein L37 |Schizosaccharomyces pombe|chr 3|||Manual	SPCC1223.05c	10 kDa	2
|rpl701||60S ribosomal protein L7|Schizosaccharomyces pombe|chr 2|||Manual	SPBC18H10.12c	29 kDa	5
|rpl1701|rpl17, rpl17-1|60S ribosomal protein L17|Schizosaccharomyces pombe|chr 2|||Manual	SPBC2F12.04	21 kDa	1
|rps1801|rps18-1|40S ribosomal protein S18 |Schizosaccharomyces pombe|chr 2|||Manual	SPBC16D10.11c	17 kDa	3

|rpl1001|rpl10-1, rpl10|60S ribosomal protein L10|Schizosaccharomyces pombe|chr 2|||Manual	SPBC18E5.04	25 kDa	1
|smd3||Sm snRNP core protein Smd3|Schizosaccharomyces pombe|chr 2|||Manual	SPBC19C2.14	11 kDa	1
|||WD repeat protein, human MAPK organizer 1 |Schizosaccharomyces pombe|chr 2|||Manual	SPBC713.05	33 kDa	1
|bip1|bip|ER heat shock protein BiP|Schizosaccharomyces pombe|chr 1|||Manual	SPAC22A12.15 c	73 kDa	3
|syf2||splicing factor, SYF2 family |Schizosaccharomyces pombe|chr 2|||Manual	SPBC3E7.13c	28 kDa	1
|rpl2802|rpl28-2, rpl28|60S ribosomal protein L27/L28|Schizosaccharomyces pombe|chr 3|||Manual	SPCC5E4.07	17 kDa	0
|cwf7|spf27|splicing factor Cwf7|Schizosaccharomyces pombe|chr 2|||Manual	SPBC28F2.04c	21 kDa	0
|rpl2502|rpl25b, rpl23a-2|60S ribosomal protein L25 |Schizosaccharomyces pombe|chr 2|||Manual	SPBC4F6.04	16 kDa	2
|rpl101|rpl1-1, rpl10a-1|60S ribosomal protein L10a|Schizosaccharomyces pombe|chr 3|||Manual	SPCC1183.08c	24 kDa	3
|rpl1502|rpl15-2|60S ribosomal protein L15b |Schizosaccharomyces pombe|chr 1|||Manual	SPAC1783.08c (+1)	24 kDa	1
|sks2|hsc1|heat shock protein, ribosome associated molecular chaperone Sks2|Schizosaccharomyces pombe|chr 2|||Manual	SPBC1709.05	67 kDa	1
|rps2302|rps23-2|40S ribosomal protein S23 |Schizosaccharomyces pombe|chr 2|||Manual	SPBP4H10.13	16 kDa	1
|rpl2701|rpl27-1|60S ribosomal protein L27|Schizosaccharomyces pombe|chr 2|||Manual	SPBC685.07c	15 kDa	2
|tef102|ef1a-b|translation elongation factor EF-1 alpha Ef1a-b|Schizosaccharomyces pombe|chr 1|||Manual	SPAC23A1.10 (+1)	50 kDa	5
|||ATP-dependent RNA helicase, spliceosomal |Schizosaccharomyces pombe|chr 1|||Manual	SPAC20H4.09	73 kDa	1
|cyp1||cyclophilin family peptidyl-prolyl cis-trans isomerase Cyp1|Schizosaccharomyces pombe|chr 1|||Manual	SPAC57A10.03	17 kDa	1

|rps1102|rps11-2, rps11|40S ribosomal protein S11 |Schizosaccharomyces pombe|chr 1|||Manual	SPAC144.11	18 kDa	2
|rps601|rps6-1|40S ribosomal protein S6|Schizosaccharomyces pombe|chr 1|||Manual	SPAC13G6.07c (+1)	27 kDa	4
|rps901|rps9-1, rps9a|40S ribosomal protein S9|Schizosaccharomyces pombe|chr 1|||Manual	SPAC24H6.07	22 kDa	1
|smd2|cwf9|Sm snRNP core protein Smd2|Schizosaccharomyces pombe|chr 1|||Manual	SPAC2C4.03c	13 kDa	4
|rps402|rps4-2|40S ribosomal protein S4 |Schizosaccharomyces pombe|chr 2|||Manual	SPBC21B10.10	30 kDa	1
|rps801|rps8-1, rps8|40S ribosomal protein S8 |Schizosaccharomyces pombe|chr 1|||Manual	SPAC2C4.16c (+1)	23 kDa	3
|rpl3201|rpl32-1|60S ribosomal protein L32|Schizosaccharomyces pombe|chr 2|||Manual	SPBC16C6.11	14 kDa	0
|cwf18||complexed with Cdc5 protein Cwf18|Schizosaccharomyces pombe|chr 3|||Manual	SPCP1E11.07c	17 kDa	2
|rpl31||60S ribosomal protein L31 |Schizosaccharomyces pombe|chr 1|||Manual	SPAC890.08	13 kDa	3
|rpl1101|rpl11-1, rpl11|60S ribosomal protein L11 |Schizosaccharomyces pombe|chr 1|||Manual	SPAC26A3.07c	20 kDa	1
|rps3||40S ribosomal protein S3 |Schizosaccharomyces pombe|chr 2|||Manual	SPBC16G5.14c	28 kDa	0
|rpl1601||60S ribosomal protein L13/L16 |Schizosaccharomyces pombe|chr 2|||Manual	SPBC839.13c	22 kDa	0
|saf4||splicing associated factor Saf4 |Schizosaccharomyces pombe|chr 2|||Manual	SPBC18H10.10 c	34 kDa	0
|rps7||40S ribosomal protein S7 |Schizosaccharomyces pombe|chr 1|||Manual	SPAC18G6.14c	22 kDa	1
|rpl14||60S ribosomal protein L14 |Schizosaccharomyces pombe|chr 1|||Manual	SPAC1805.13	15 kDa	2
|rps2||40S ribosomal protein S2 |Schizosaccharomyces pombe|chr 3|||Manual	SPCC576.08c	28 kDa	2
|rps2602|rps26-2|40S ribosomal protein S26 |Schizosaccharomyces pombe|chr 1|||Manual	SPAC1805.11c	14 kDa	2
|rps1501|rps15-1|40S ribosomal protein S15 |Schizosaccharomyces pombe|chr 3|||Manual	SPCC1393.03	18 kDa	3

|rpl702|rpl7-2, rpl7, rpl7b|60S ribosomal protein L7|Schizosaccharomyces pombe|chr 1|||Manual	SPAC3H5.07	28 kDa	1
|smb1|smb|Sm snRNP core protein Smb1|Schizosaccharomyces pombe|chr 1|||Manual	SPAC26A3.08	15 kDa	4
|sum3|ded1, slh3, moc2|ATP-dependent RNA helicase Sum3|Schizosaccharomyces pombe|chr 3|||Manual	SPCC1795.11	70 kDa	3
|rps2502|rps25-2, rps25|40S ribosomal protein S25 |Schizosaccharomyces pombe|chr 1|||Manual	SPAC694.05c (+1)	10 kDa	1
|rpl24||60S ribosomal protein L24 |Schizosaccharomyces pombe|chr 1|||Manual	SPAC6G9.09c (+1)	17 kDa	3
|smd1||Sm snRNP core protein Smd1|Schizosaccharomyces pombe|chr 1|||Manual	SPAC27D7.07c	13 kDa	0
|rpl2101|rpl21, rpl21-1|60S ribosomal protein L21 |Schizosaccharomyces pombe|chr 2|||Manual	SPBC365.03c	18 kDa	0
|rps502|rps5-2|40S ribosomal protein S5 |Schizosaccharomyces pombe|chr 1|||Manual	SPAC328.10c	22 kDa	0
|rpl3802|rpl38-2, rps38|60S ribosomal protein L38 |Schizosaccharomyces pombe|chr 1|||Manual	SPAC30D11.12	8 kDa	0
|rpl1201|rpl12-1, rpl12.1|60S ribosomal protein L12.1/L12A|Schizosaccharomyces pombe|chr 3|||Manual	SPCC16C4.13c	18 kDa	1
|rps2401|rps24-1, rps24|40S ribosomal protein S24 |Schizosaccharomyces pombe|chr 1|||Manual	SPAC17G6.06	15 kDa	1
|rpl22|SPAP8A3.01|60S ribosomal protein L22 |Schizosaccharomyces pombe|chr 1|||Manual	SPAC11E3.15	13 kDa	2
|rps1401|rps14-1, rps14|40S ribosomal protein S14 |Schizosaccharomyces pombe|chr 1|||Manual	SPAC3H5.05c	15 kDa	2
|bis1||stress response protein Bis1|Schizosaccharomyces pombe|chr 3|||Manual	SPCC364.02c	43 kDa	0
|rpl3401|rpl34, rpl34-1|60S ribosomal protein L34|Schizosaccharomyces pombe|chr 1|||Manual	SPAC23A1.08c	13 kDa	1
|rpl1801|rpl18-1, rpl18|60S ribosomal protein L18|Schizosaccharomyces pombe|chr 2|||Manual	SPBC11C11.07	21 kDa	1

|rps1502|rps15-2, rps15|40S ribosomal protein S15 |Schizosaccharomyces pombe|chr 1|||Manual	SPAC1071.07c	18 kDa	2
|||pyruvate decarboxylase |Schizosaccharomyces pombe|chr 1|||Manual	SPAC1F8.07c	62 kDa	1
|rpl2702|rpl27-2|60S ribosomal protein L27 |Schizosaccharomyces pombe|chr 3|||Manual	SPCC74.05	15 kDa	0
|cwf14||G10 protein|Schizosaccharomyces pombe|chr 2|||Manual	SPBC24C6.11	17 kDa	0
|rps2201|rps22-1, rps15a-1|40S ribosomal protein S15a |Schizosaccharomyces pombe|chr 1|||Manual	SPAC22A12.04c	15 kDa	0
|rpl35a|rpl33|60S ribosomal protein L35a|Schizosaccharomyces pombe|chr 3|||Manual	SPCP31B10.08c	12 kDa	0
|rpl4301|rpl43-1, rpl43, rpl37a-1|60S ribosomal protein L37a |Schizosaccharomyces pombe|chr 2|||Manual	SPBC800.04c (+1)	10 kDa	0
|rps3001|rps30-1|40S ribosomal protein S30 |Schizosaccharomyces pombe|chr 1|||Manual	SPAC19B12.04	7 kDa	1
|rpl401|rpl4-1, rpl4|60S ribosomal protein L2 |Schizosaccharomyces pombe|chr 2|||Manual	SPBC1711.06	40 kDa	1
|||ribomal-ubiquitin fusion protein Ubi5 |Schizosaccharomyces pombe|chr 1|||Manual	SPAC589.10c (+1)	17 kDa	2
|rps1602|rps16-2, rps16|40S ribosomal protein S16 |Schizosaccharomyces pombe|chr 1|||Manual	SPAC664.04c	15 kDa	1
|rps101|rps1-1, rps3a-1|40S ribosomal protein S3a|Schizosaccharomyces pombe|chr 1|||Manual	SPAC13G6.02c	28 kDa	1
|fib1|fib|fibrillarin|Schizosaccharomyces pombe|chr 2|||Manual	SPBC2D10.10c	32 kDa	2
|act1|cps8|actin Act1|Schizosaccharomyces pombe|chr 2|||Manual	SPBC32H8.12c	42 kDa	1
|mlo3||RNA binding protein Mlo3|Schizosaccharomyces pombe|chr 2|||Manual	SPBC1D7.04	22 kDa	1
|dbp2||ATP-dependent RNA helicase Dbp2|Schizosaccharomyces pombe|chr 2|||Manual	SPBP8B7.16c	62 kDa	1
|hsp90|swo1, git10|Hsp90 chaperone|Schizosaccharomyces pombe|chr 1|||Manual	SPAC926.04c	81 kDa	1

|rpp201|rpp2, rpp2-1|60S acidic ribosomal protein P2A subunit |Schizosaccharomyces pombe|chr 2|||Manual	SPBP8B7.06	11 kDa	1
|lea1||U2 snRNP-associated protein Lea1 |Schizosaccharomyces pombe|chr 2|||Manual	SPBC1861.08c	27 kDa	0
|rpp0||60S acidic ribosomal protein Rpp0 |Schizosaccharomyces pombe|chr 3|||Manual	SPCC18.14c	34 kDa	0
|rpl1702|rpl17-2, rpl17|60S ribosomal protein L17 |Schizosaccharomyces pombe|chr 3|||Manual	SPCC364.03	21 kDa	1
|leu1|SPBC1E8.07c|3-isopropylmalate dehydrogenase Leu1|Schizosaccharomyces pombe|chr 2|||Manual	SPBC1A4.02c	40 kDa	0
|eno101|eno1|enolase |Schizosaccharomyces pombe|chr 2|||Manual	SPBC1815.01	47 kDa	0
|rps1702|rps17-2, rps17|40S ribosomal protein S17 |Schizosaccharomyces pombe|chr 3|||Manual	SPCC24B10.09	16 kDa	0
|||human leukocyte receptor 1 ortholog|Schizosaccharomyces pombe|chr 3|||Manual	SPCC5E4.10c	24 kDa	1
|bag101|bag1-a, bag1|BAG family molecular chaperone regulator Bag101 |Schizosaccharomyces pombe|chr 2|||Manual	SPBC16G5.11c	22 kDa	0
|nxt3|glp1|ubiquitin protease cofactor Glp1 |Schizosaccharomyces pombe|chr 2|||Manual	SPBP8B7.11	48 kDa	0
|rpl2801|rpl28-1|60S ribosomal protein L27/L28|Schizosaccharomyces pombe|chr 2|||Manual	SPBC776.11	17 kDa	0
|rpl901|rpl9-1|60S ribosomal protein L9|Schizosaccharomyces pombe|chr 1|||Manual	SPAC4G9.16c	22 kDa	0
|gar2||nucleolar protein required for rRNA processing|Schizosaccharomyces pombe|chr 1|||Manual	SPAC140.02	53 kDa	0
|ssa1||heat shock protein Ssa1 |Schizosaccharomyces pombe|chr 1|||Manual	SPAC13G7.02c	70 kDa	4
|tif471||translation initiation factor eIF4G|Schizosaccharomyces pombe|chr 1|||Manual	SPAC17C9.03	154 kDa	0
|rpl42|rpl36a|60S ribosomal protein L36/L42|Schizosaccharomyces pombe|chr 1|||Manual	SPAC15E1.03	12 kDa	0

|||human LYHRT homolog|Schizosaccharomyces pombe|chr 2|||Manual	SPBC215.06c	20 kDa	3
|||ribosome biogenesis ATPase, Arb family ABCF1-like |Schizosaccharomyces pombe|chr 3|||Manual	SPCC825.01	93 kDa	2
|eft201|eft2-1, etf2, SPAPYUK71.04c|translation elongation factor 2 |Schizosaccharomyces pombe|chr 1|||Manual	SPAC513.01c	93 kDa	0

VIII.2 Publications

Aronica, L., Kasparek, T., **Ruchman, D**., Marquez, Y., Cipak, L., Cipakova, I., Anrather, D., Mikolaskova, B., Radtke, M., Sarkar, S. et al. (2015). The spliceosome-associated protein Nrl1 suppresses homologous recombination-dependent R-loop formation in fission yeast. Nucleic Acids Research